

Structural Vulnerability Profile (SVP) Radiograph Guide

Version 1. 18 October 2023

Aliana Schwartz, Emily Romdenne, K. Kirk, and Taylor Perritt

[The UWF Biocultural Research Laboratory](#)

Department of Anthropology, University of West Florida
11000 University Parkway, Building 13, Room 307, Pensacola, FL 32514

Biocultural Laboratory Faculty:

Allysha P. Winburn, PhD, RPA, D-ABFA—awinburn@uwf.edu

Katherine A. Miller Wolf, PhD, RPA—kmillerwolf@uwf.edu

Meredith G. Marten, PhD, MPH—mmarten@uwf.edu

How to cite:

Schwartz, A., Romdenne, E., Kirk, K. & Perritt, T. (2023). Structural Vulnerability Profile (SVP) Radiograph Guide. Version 1. A working document of the *University of West Florida Biocultural Research Laboratory*, Pensacola, FL.

SVP Radiograph Guide: Table of Contents

Note that the below categories (e.g., Dental, Cranial) correspond with the UWF Biocultural Lab's SVP data-collection spreadsheets, and the numbered subcategories correspond with traits scored per our data-collection protocol. Please contact Biocultural Lab faculty if you wish to share our data-collection sheets.

Dental	5
1. Abscesses	5
2. Carious Lesions	6
3. Dental Enamel Defects	6
4. Restorations	7
5. Implants	8
6. Paramasticatory Wear	9
7. Abfractions/NCCLs/Cervical Lesions:	10
8. Dental Calculus	10
9. Alveolar Bone Loss	11
10. Alveolar Bone Deposition	12
11. Staining	12
12. Teeth Absent	12
Cranial	13
13. Cleft Palate	13
14. Cranial Lesions	14
15. Mastoiditis	14
16. Stellate Scarring	15
Postcranial	16
17. Periosteal New Bone Lesions	16
18. Osteomyelitis	16
19. Proliferative Activity	17
20. Lytic Activity	17
21. Deformative	18
22. Enthesopathies	19
Ossification at insertion site	19
Excavation at insertion site	19

Ossification of connective tissue	20
23. Osteoarthritis	20
Osteophytes	20
Osteophytes and sclerotic activity	20
Porosity/Erosion	21
Sclerosis	21
Eburnation	21
24. Vertebral Osteoarthritis	22
Zygapophyses/Intervertebral facets	22
Centrum	22
Spinous processes	23
Transverse processes	23
25. Schmorl's Nodes	23
26. Spina Bifida	24
27. Ankylosing Spondylitis	24
28. Curvature of Spine	26
Scoliosis	26
Cervical Lordosis	26
Thoracic Kyphosis	26
Lumbar Lordosis	27
29. Atherosclerosis Calcification	28
30. Pleural Rib Lesions	28
Trauma and Surgery	29
31. Fractures	29
Types of Fractures	29
Antemortem/Perimortem	31
32. Dislocations	32
33. Surgical Intervention	33
Standards	36
34. Craniofacial Asymmetry	36
35. Basion-Bregma Height	36
36. Maximum Fibula Length	36
37. Femur Midshaft Diameter	37

38. Pubic Symphysis (Brooks and Suchey 1990)	37
39. Acetabular Rim Traits (SanMillán et al., 2017)	38
40. Fourth Sternal Rib Ends	40
Standards for (White) Males (Işcan et al., 1984)	40
Standards for (White) Females (Işcan et al., 1985)	42
41. Vertebral Neural Canal Dimensions	43

Dental

1. Abscesses

Alternate name(s): periapical abscess, endodontal disease.

Definition(s): Abscesses indicate pulp chamber inflammation following excessive attrition or dental caries...abscesses can be identified by the presence of a drainage channel leading from the apex of the tooth through the alveolar bone (Buikstra and Ubelaker, 1994, p. 55).

Not visible within the first ten days radiographically. Diagnostically, they are a well-defined radiolucency at/below the root apex, usually <10 mm. May have a surrounding zone of sclerosis (condensing osteitis) centered over the root apex of teeth with endodontal or periodontal disease. Sclerotic lesion will be <22 mm (Abrahams, 2001).

“Radiographs show that inflammation may remain at a low level for years, with the only sign a widening of periodontal ligament space and the formation of a sclerotic zone of thickened bone trabeculae, with no sign of swelling on the jaw surface. A periapical granuloma is usually diagnosed when a radiolucency (diffuse or sharply defined) involves loss of the lamina dura around the root apex...Radiographically, there may be little evidence of rapidly formation abscess.” (Hillson, 1996, p. 284-285)

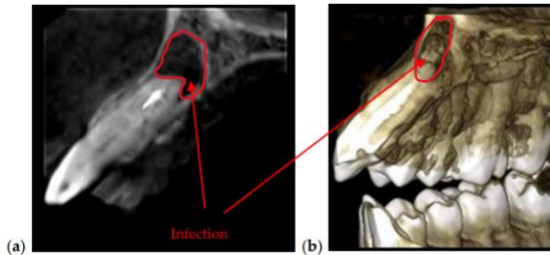


Figure 4. (a) Sagittal view and (b) 3D CBCT reconstruction of an infection formed at the tip of a tooth. Patient C.B.G., female, age 37 years, diagnosed with dental abscess.

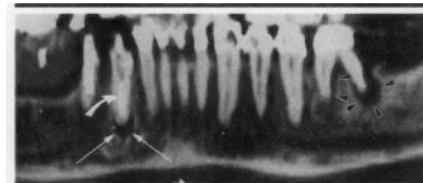


Figure 6. Panoramic dental CT scan in a 60-year-old man with advanced periodontal (arrowheads) and endodontal (straight arrows) lesions. Note how periodontal disease travels down the sides of the root, while endodontal disease affects the root apex. A radiopaque post from a root canal procedure is seen in a tooth with an endodontal lesion (curved arrow). (Reprinted, with permission, from reference 14.)

Image source(s): Left - Scheinfeld et al., 2012, Figure 4; Right - Abrahams, 2001, Figure 6

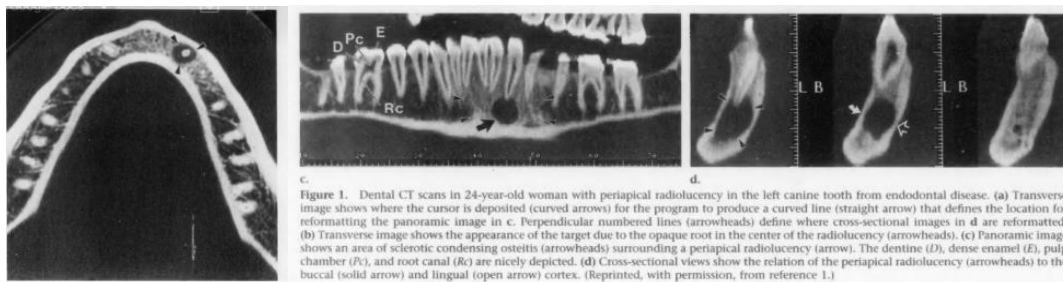


Figure 1. Dental CT scans in 24-year-old woman with periapical radiolucency in the left canine tooth from endodontal disease. (a) Transverse image shows where the cursor is deposited (curved arrows) for the program to produce a curved line (straight arrow) that defines the location for reformatting the panoramic image in c. Perpendicular numbered lines (arrowheads) define where cross-sectional images in d are reformatted. (b) Transverse image shows the appearance of the target due to the opaque root in the center of the radiolucency (arrowheads). (c) Panoramic image shows an area of sclerotic condensing osteitis (arrowheads) surrounding a periapical radiolucency (arrow). The dentine (D), dense enamel (E), pulp chamber (Pc), and root canal (Rc) are nicely depicted. (d) Cross-sectional views show the relation of the periapical radiolucency (arrowheads) to the buccal (solid arrow) and lingual (open arrow) cortex. (Reprinted, with permission, from reference 1.)

Image source(s): Abrahams, 2001, Figure 1

2. Carious Lesions

Alternate names(s): caries, cavities

Definition(s): “Caries are detectable as radiolucency in dental x-rays, but this is not a sensitive technique, and spot lesions are seen at the surface before they are recognizable radiographically.” (Hillson, 1996, p. 269)

“... in radiography, the complex folds of enamel in the occlusal surface mask most enamel lesions, so that radiolucency is apparent only when the dentine is affected (van Amerongen et al., 1992; Espelid et al., 1994; Goaz & White, 1994).” (Hillson, 1996, p. 272)

“In dental radiographs, root caries lesions that have penetrated the CDJ are seen in the dentine as scooped radiolucencies (Goaz & White, 1994) that can be difficult to distinguish from cervical burnout (p. 13).” (Hillson, 1996, p. 275)

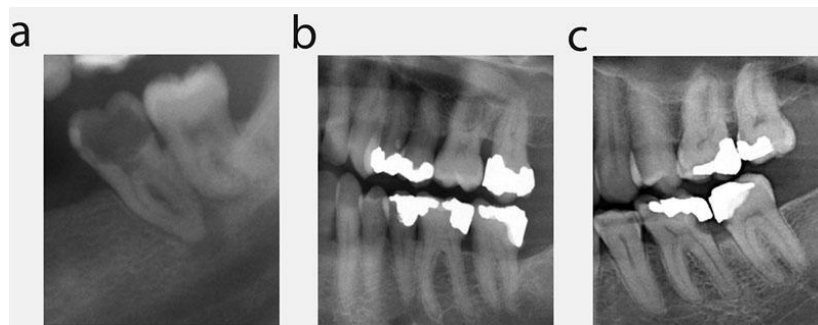


Image source(s): Masthoff et al., 2018, Figure 2: Opacity in radiographs and guide under FDI dental notation. a) Extensive caries lesion with lucency of the corona. Apical lucency is also suspicious of a consecutive apical periodontitis with typical osteolysis. b) Sufficient fillings of multiple teeth in line with the margin of the teeth. c) Insufficient fillings with secondary caries at 27, 36 and 37 with a lucency close to the filling edges, which protrude in case of 36 and 37. This is a risk factor for accumulation of food rest, resulting in a higher risk of secondary caries lesions. (https://en.wikipedia.org/wiki/Dental_notation)

3. Dental Enamel Defects

Alternate name(s): linear enamel hypoplasias, hypoplasias, hypoplastic defects, hypomineralization

Definition: hypoplasias are deficiencies in enamel thickness which may be caused by three phenomena: systemic metabolic stress, hereditary anomalies, and local trauma (Buikstra and Ubelaker, 1994, p. 56).

Different types are difficult to tell apart, but they depend on the time of dental development (e.g. either during matrix creation or afterward, during calcification or maturation).

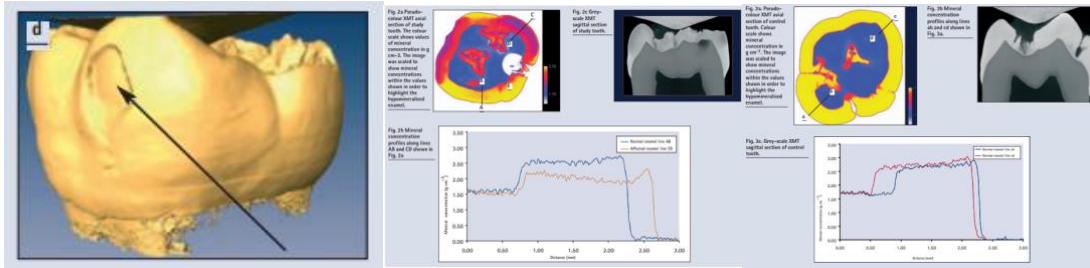


Image source(s): Fearne et al., 2004; Left - Figure 1d: Surface-rendered view of regions of lower mineral concentration; Center and Right - Figure 2 and 3: Enamel defects with hypomineralized regions, along with their markedly different spectrographic absorption.

4. Restorations

Treated abscesses (root canal): “The apical foramen and root canal are sealed with a radiopaque material called gutta-percha that causes the normally radiolucent pulp chamber to appear radiopaque on the images.” (Abrahams, 2001, p. 340)

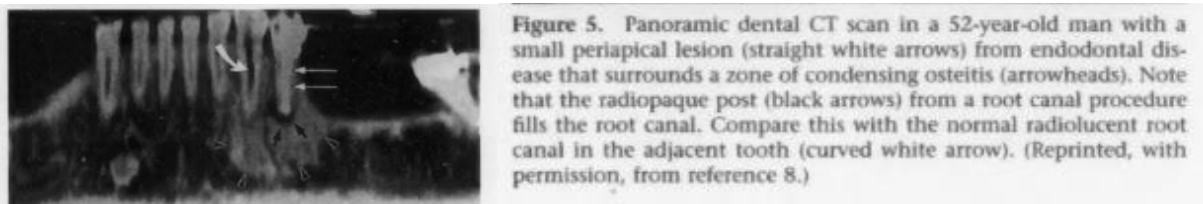


Image source(s): Abrahams, 2001, Figure 5

Filled cavities

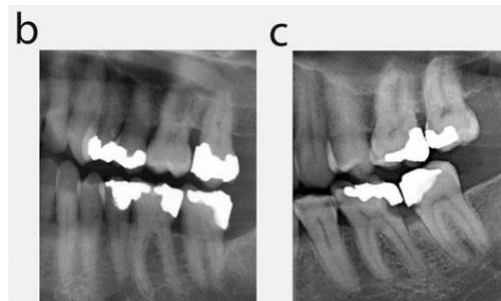


Image source(s): Masthoff et al., 2018, Figure 2: b) Sufficient fillings of multiple teeth in line with the margin of the teeth. c) Insufficient fillings with secondary caries at 27, 36 and 37 with a lucency close to the filling edges, which protrude in case of 36 and 37. This is a risk factor for accumulation of food rest, resulting in a higher risk of secondary caries lesions.

5. Implants

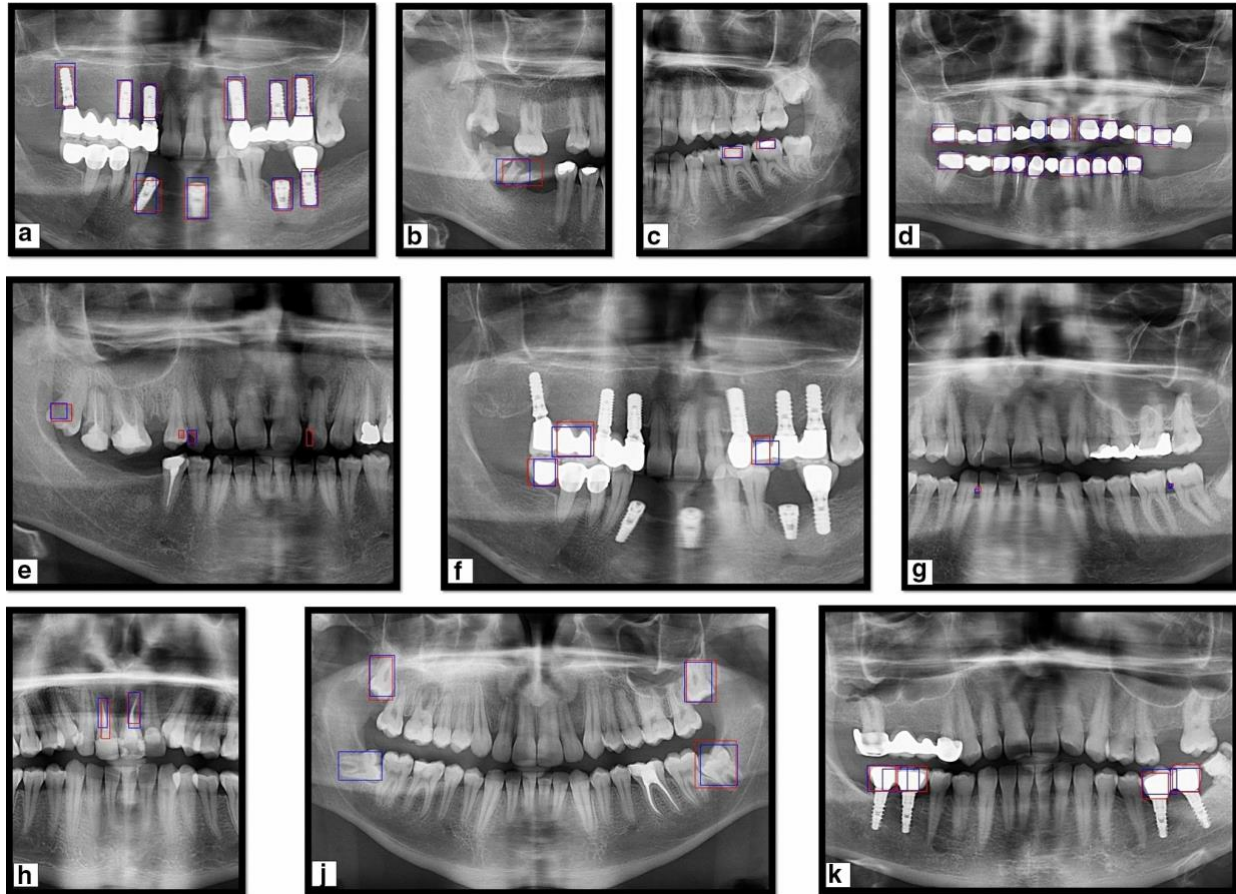


Image source(s): Basaran et al., 2022, Figure 1: The results for detecting dental conditions in panoramic radiographs with AI models (a) implant (b) residual root (c) filling (d) crown (e) caries (f) pontic (g) dental calculus (h) root-canal treated tooth (j) impacted tooth (k) implant-supported crown.

Braces



Image source(s): [Radiopaedia](#): Braces on the central maxillary incisors and the left lateral maxillary incisor in an individual with cleft palate.

Dentures



Image source(s): Otsuka et al., 2007, Figure 6b: Dental denture artifact on CT image. The energy of positron is much higher than X ray, thus PET data is overestimated. Tongue cancer is unclear in attenuation-corrected PET Image, but it is clearly demonstrated in non attenuated-corrected PET image.

Veneers

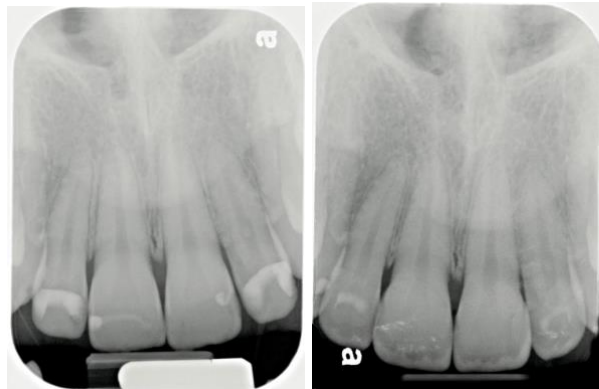


Image source(s): Notarantonio, 2011, Figure 3 & 13: Pre and post x-rays, respectively, of veneer modification.

6. Paramasticatory Wear

Definition(s): Dentists classify this as attrition, which is the wear of the occlusal, incisal, or interproximal surfaces of the teeth is produced by interaction and friction between maxillary and mandibular teeth. There's also wear in between teeth (abrasion).

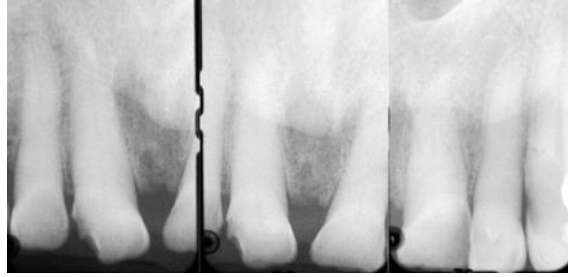


Image source(s): Lam, 2009, Figure 10.2: On the radiograph, attrition is viewed as a mild wear of incisal and occlusal surfaces of teeth involved. Depending on the stage of the wear, the crown looks shorter, and volume of the pulp declines due to the deposition of secondary dentine or of amorphous dentine with age (Ketterl, 1983). Widening of periodontal ligament (PDL), the soft connective tissue between the inner wall of the alveolar socket and the roots of the teeth, can be seen if the tooth is mobile and occasionally there is evidence of hypercementosis.

7. Abfractions/NCCLs/Cervical Lesions:

Definition(s): Non-carious cervical lesions (NCCLs) [are] characterized by the loss of hard tissue at the cemento-enamel junction (CEJ) in the absence of caries (Hur et al., 2011, p. 469). Characterized by sharp enamel margins at the coronal margins of defects.

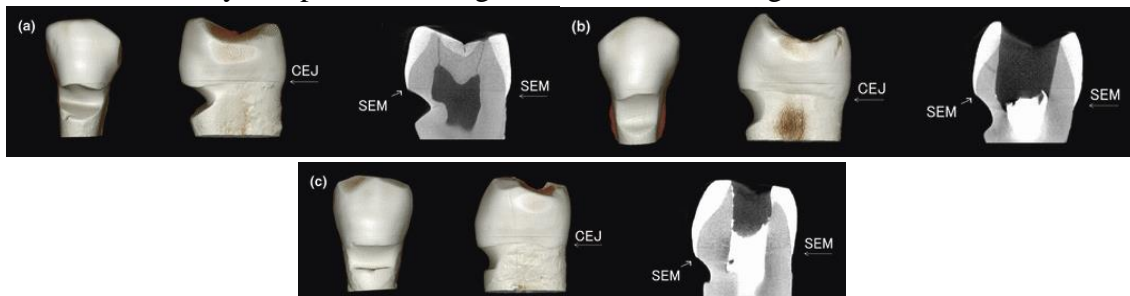


Image source(s): Hur et al., 2011, Figure 2: Representative samples of three types of the lesions: (a) wedge-shaped lesion, (b) saucer-shaped lesion and (c) mixed shape lesion. Left column shows mid-buccal aspect, mid column shows proximal aspect and the right column shows buccolingual longitudinal sectional images. Sectional images show the intact sharp enamel margins (SEM) at coronal margins of the lesions.

8. Dental Calculus

Definition(s): Dental calculus is calcified bacterial plaque that forms throughout an individual's life on the subgingival and/or supragingival tooth surfaces...underneath a layer of nonmineralized plaque...The boundary between dental calculus and enamel or dentin is strong. There is bonding and sometimes complete fusion between the calculus and tooth apatite or enamel crystals...and residue may remain adhering to the teeth even after cleaning.” (*Ortner's Paleopathology*, Buikstra, 2019, p. 778)

“...average sensitivity of digital radiography was 50%, average specificity was 82.2%, PPV was 94%, and NPV 23.2%. A threshold of >30% of interproximal root surface covered with

calculus and increasing size of deposits were associated with improved detection ($P < 0.05$).” (Hyer et al., 2020)

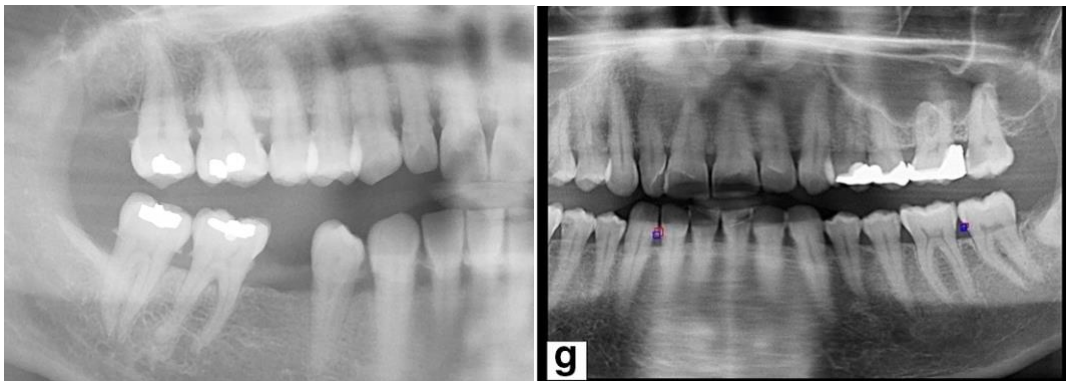


Image source(s): Left - Korostoff et al., 2016: teeth 18, 28, 35, 38, 45 and 48 are absent (based on the FDI World Dental Federation notation). Previous dental restorations noted to most of the remaining molar teeth. No periapical lucency identified in the right half of the mandible. Minor increase in the periodontal space of 34. No dental caries appreciated. Extensive calculus disease at the gumline causing small radiopaque spurs on the surface of the teeth.; Right - Basaran et al., 2022, Figure 1: The results for detecting dental conditions in panoramic radiographs with AI models... (g) dental calculus....

9. Alveolar Bone Loss

Alternate name(s): periodontitis; periodontal disease

Definition(s): Periodontitis “is initiated by polymicrobial plaque, biofilm, or abrasive effects of calculus, which are associated with the build-up of plaque. The build-up of plaque then causes an inflammatory response in the periodontal tissues of the teeth... manifesting as porosity, alveolar bone loss, and the development of pocketing or recessing, both vertical and horizontal, around the roots as the bone is resorbed.” (*Ortner’s Paleopathology*, Kinaston et al., 2019:771)

Radiographic threshold of bone loss set at least 10% of root length. Some authors suggest using a staged assessment of periodontitis based on the extent and severity, i.e., severity/disease progression (Savage et al., 2009).

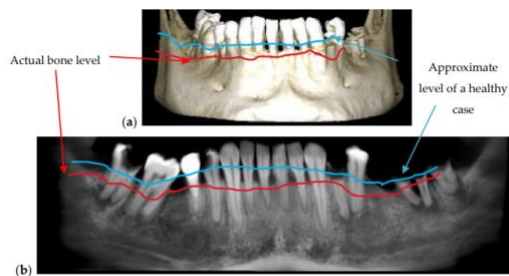


Figure 5. Periodontitis disease observed on a 3D CBCT reconstruction (a) and on a panoramic radiography (b). Patient C.O., male, age 34 years, diagnosed with periodontitis, alongside other dental issues such as cavities and dental abscesses.

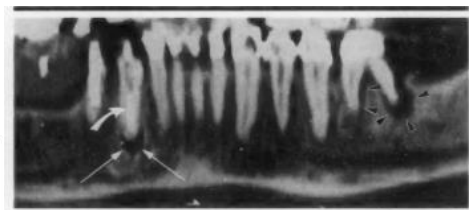


Figure 6. Panoramic dental CT scan in a 60-year-old man with advanced periodontal (arrowheads) and endodontal (straight arrows) lesions. Note how periodontal disease travels down the sides of the root, while endodontal disease affects the root apex. A radiopaque post from a root canal procedure is seen in a tooth with an endodontal lesion (curved arrow). (Reprinted, with permission, from reference 14.)

Image source(s): Left - Erdelyi et al., 2020, Figure 5; Right - Abrahams, 2001, Figure 6

10. Alveolar Bone Deposition

Includes: filling in of alveolar crypts after antemortem tooth loose, proliferative lesions, odontogenic tumors made of bone, etc.

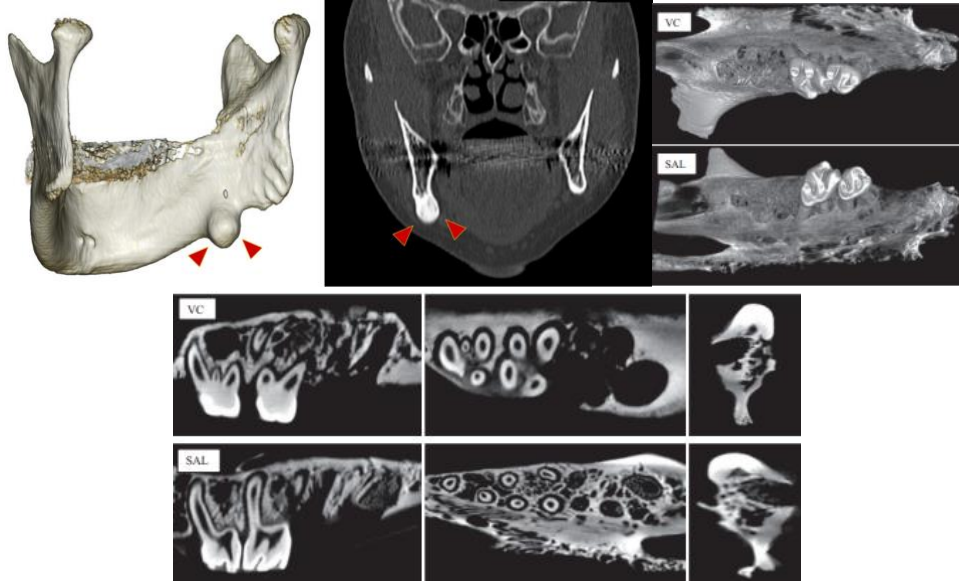


Image source(s): Top Left and Bottom - Chen et al., 2020; Top Right - Kamimura et al., 2020

11. Staining

Not visible radiographically

12. Teeth Absent



Image source(s): Left - Korostoff et al., 2016: teeth 18, 28, 35, 38, 45 and 48 are absent (based on the FDI World Dental Federation notation). Previous dental restorations noted to most of the remaining molar teeth. No periapical lucency identified in the right half of the mandible. Minor increase in the periodontal space of 34. No dental caries appreciated. Extensive calculus disease at the gumline causing small radiopaque spurs on the surface of the teeth; Right - [Radiopaedia](#): Congenitally absent lateral incisors.

Cranial

13. Cleft Palate

Definition(s): Cleft lip and cleft palate are openings or splits in the upper lip, the roof of the mouth (palate) or both. Cleft lip and cleft palate result when facial structures that are developing in an unborn baby don't close completely ([Mayo Clinic](#)).

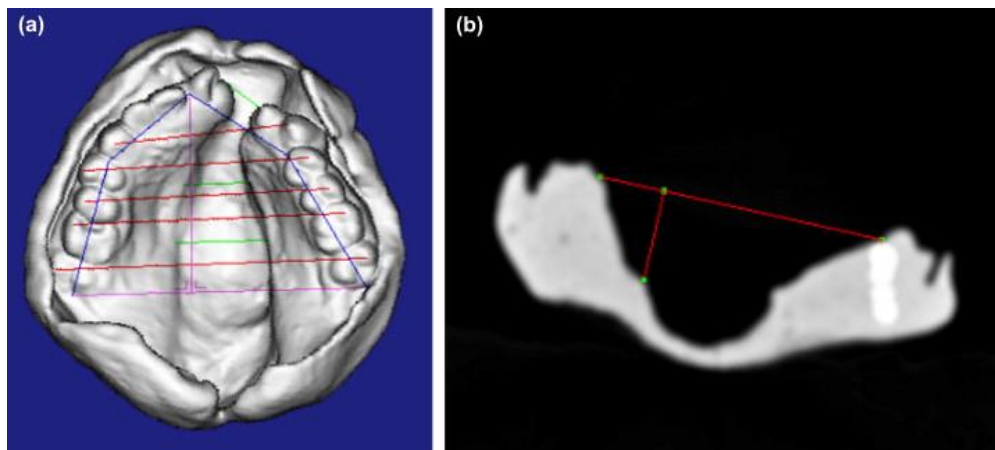


Image source(s): Diah et al., 2007, Figure 1: Linear dental measurement. Interdental distances, arch length, arch depth and cleft widths (a) and palatal vault depth (b). In (a), the transverse lines show linear distances between canines, first premolars, second premolars, first molars and second molars. The peripheral connected line represents arch length. The perpendicular line crossing sagittally from the inter-incisivus point to the line connecting the most distal part of the second molar represents the arch depth. The central lines represent the cleft width at the alveolar level, premolar and molar levels. In (b), palatal vault depth, as presented in the picture, is the line perpendicular from the most medial point of the deepest part of the palate to the line interconnecting the alveolar ridge of both sides.

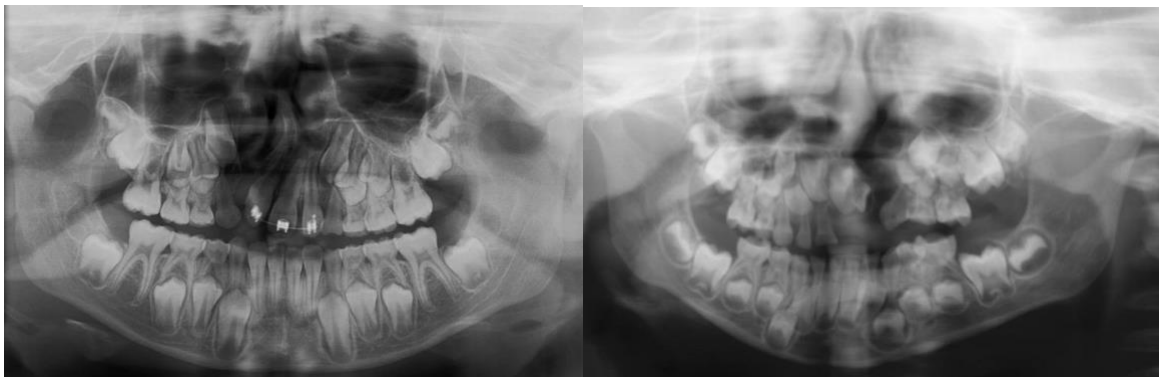


Image source(s): [Radiopaedia left](#), [right](#)

14. Cranial Lesions

Includes: Cribriform orbitalia, porotic hyperostosis, hyperostosis frontalis interna, and other porotic, proliferative, and lytic lesions on the cranium.

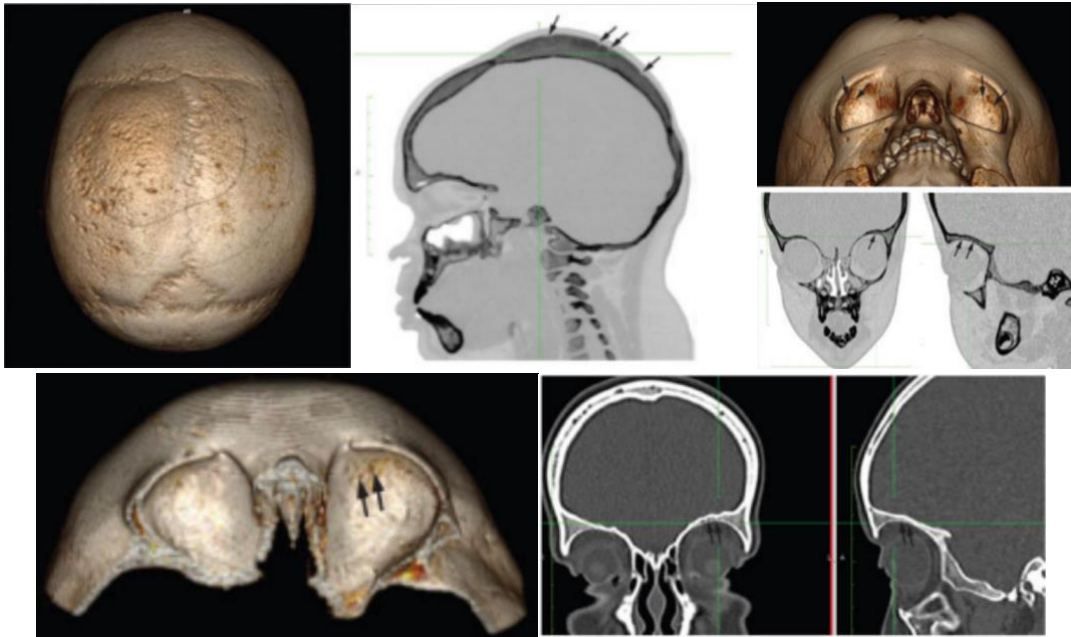


Image source(s): O'Donnell et al., 2020

15. Mastoiditis

Alternate name(s): Acute mastoid osteitis

Definition(s): Acute coalescent mastoiditis is defined by the acute form of destruction of the thin bony septae between mastoid air cells. It may be followed by the formation of abscess cavities and the dissipation of pus into adjacent areas. For our purposes, the mastoiditis will have to be severe enough that one could see a bulging or cavity formation of the temporal bone and/or petrous portion.

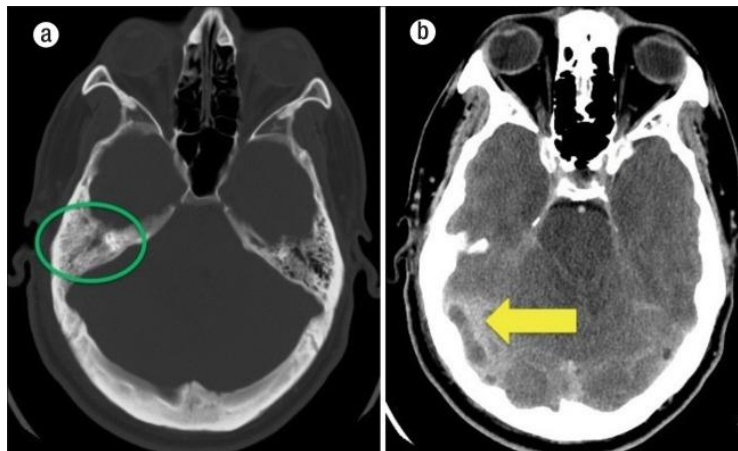


Image source(s): Levine et al., 2012, Figure 1: CT scans of the patient showing (a) right mastoid air cell opacification (green circle) and (b) in the contrast-enhanced image, dural sinus thrombosis (yellow arrow) and surrounding inflammatory and edematous changes.

16. Stellate Scarring

Definition(s): Stellate scar sign is defined as the centrally-placed, well-defined, stellate area of low density on computed tomography (CT) appearance of solid tumors. Radiating and asterisk-like fracture to the skull, usually on the parietal(s).

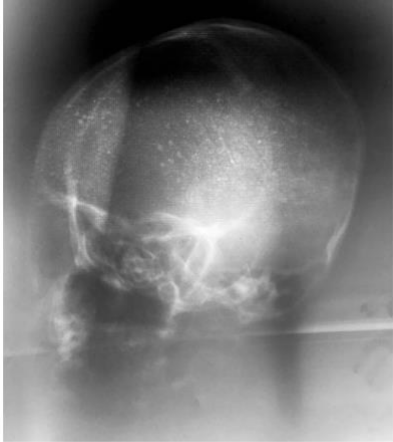


Figure 3: Lateral head X-ray. No other imaging modalities were available or functional at time of patient presentation.

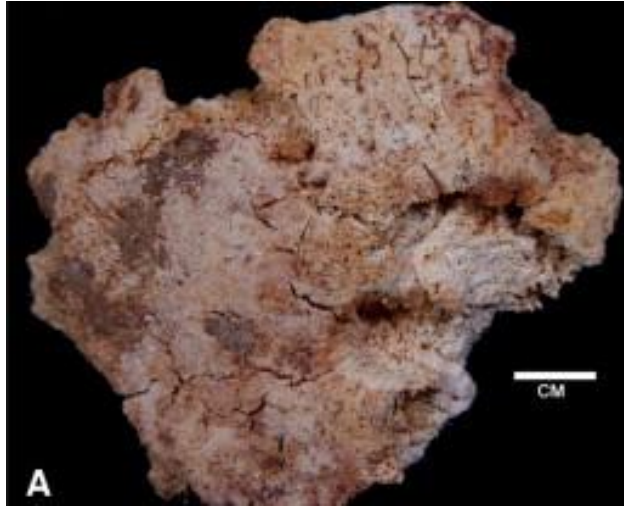


Image source(s): Left - Klaus and Ortner, 2014; Right - Kim et al., 2019

Postcranial

17. Periosteal New Bone Lesions

Definition(s): “Periosteal reactions need to be ossified to be detectable radiographically, which typically takes between 10 days to 3 weeks following insult.” (Wenaden et al., 2005)



Image source(s): Left - Paja et al., 2012; Right - Bissetet et al., 2014: Spiculated periosteal new bone growth.

18. Osteomyelitis

Definition(s): Osteomyelitis is an inflammatory condition that begins in the marrow spaces of bone and primarily affects the inner (endosteal) surface... The distinction between osteomyelitis and periostosis cannot always be made in dry bones. However, in periostosis there will be no cloacae, involucrum, or changes in the marrow cavity. Furthermore, pathological periosteal bone tends to be superficial to the normal cortex, at least in the early stages of the disease causing it (*Ortner's Paleopathology*, Buikstra, 2019, p. 287 & 292).



Image source(s): Left - Strickland, 2014; Center and Right - Bissetet et al., 2014

19. Proliferative Activity

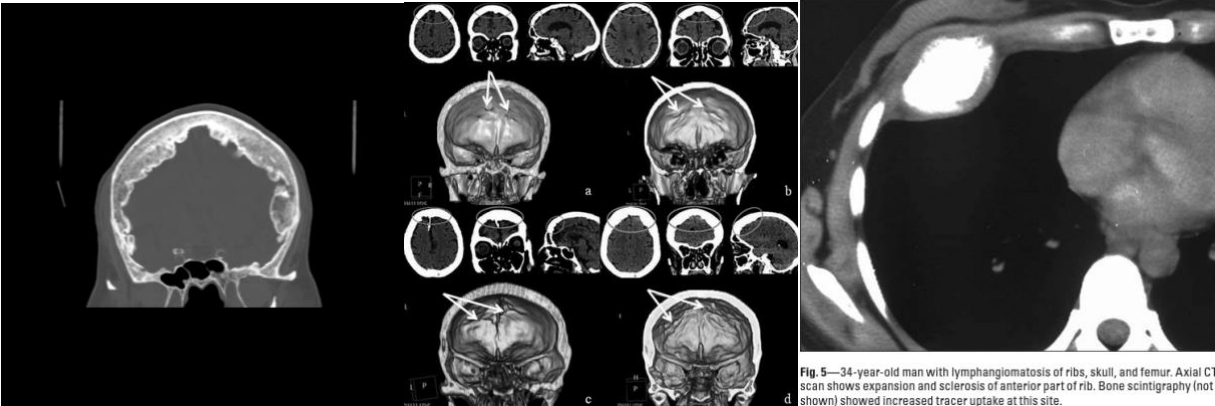


Fig. 5—34-year-old man with lymphangiomatosis of ribs, skull, and femur. Axial CT scan shows expansion and sclerosis of anterior part of rib. Bone scintigraphy (not shown) showed increased tracer uptake at this site.

Image source(s): Left - [Radiopaedia](#); Center - May et al., 2010; Right - Levine et al., 2009

20. Lytic Activity

Usually show a lower density or attenuation than the normal cancellous bone on radiographs due to its composition of fatty liquid and solid soft tissue components.



Image source(s): Radiopaedia - [Left](#), [Center Left](#), [Center Right](#), [Right](#)



Image source(s): AlShati et al., 2013: (a) Lesions on the left scapula, (e) T4 vertebrae, and (f) manubrium.



Image source(s): Strickland, 2014

21. Deformative

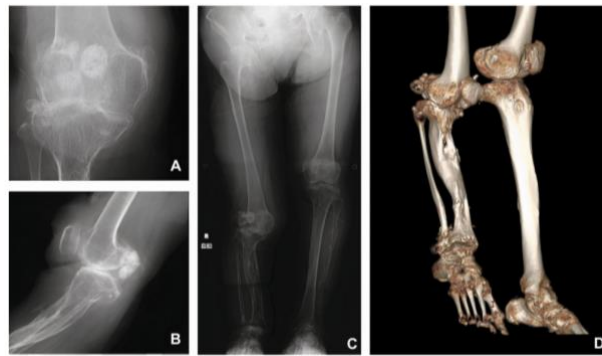


Image source(s): Balaji et al., 2021



Image source(s): Radiopaedia - [Left](#), [Center](#), [Right](#)

22. Enthesopathies

Definition(s): “Enthesopathies also occur at sites of tendon and ligament insertion...[regarding t]he pathogenesis of enthesopathy...the bony projections are probably the result of repeated hard use of the muscle over a relatively long duration of time rather than from a single traumatic event” (*Ortner’s Paleopathology*, Buikstra, 2019, p. 258).

“Enthesophytes...are projections or spicules of bones at sites of tendinous or ligamentous attachments” (Buikstra and Ubelaker, 1994, p. 119).

Ossification at insertion site



Image source(s): Left - Slonimksy et al., 2016; Center - Ikeguchi et al., 2022; Right - [Radiopaedia](#)

Excavation at insertion site

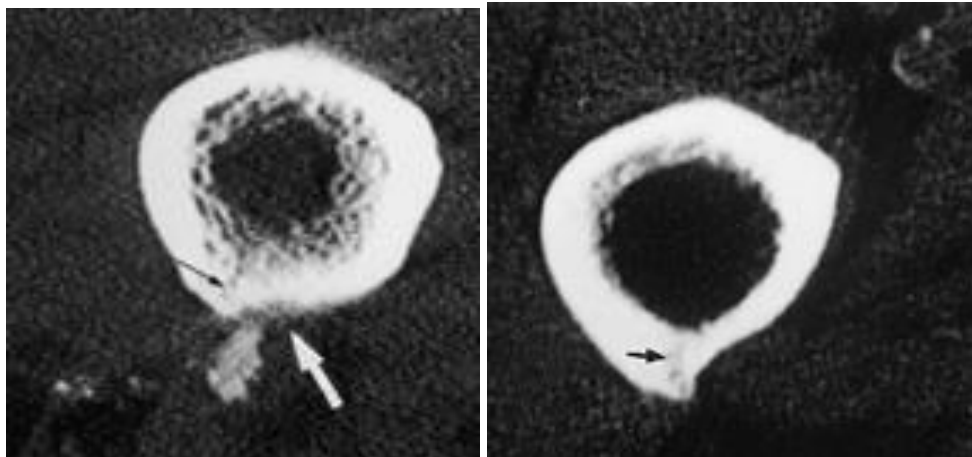


Image source(s): Hottat et al., 1998: Left - Arrow pointing to a well defined excavation site on the femoral enthesis for the gluteus maximus in a symptomatic patient; Right - Arrow pointing to a poorly defined excavation site on the same enthesis in an asymptomatic patient.

Ossification of connective tissue



Image source(s): Verlaan et al., 2007: Arrows point to ossification of flavum ligament.

23. Osteoarthritis

Definition(s): “Typical features of osteoarthritis include lipping (bony spur or osteophytic development) marginal to the articular surface, porosity of the surface, and eburnation...the bone-on-bone polish that develops following cartilage degeneration” (Buikstra and Ubelaker, 1994, p. 112).

Osteophytes

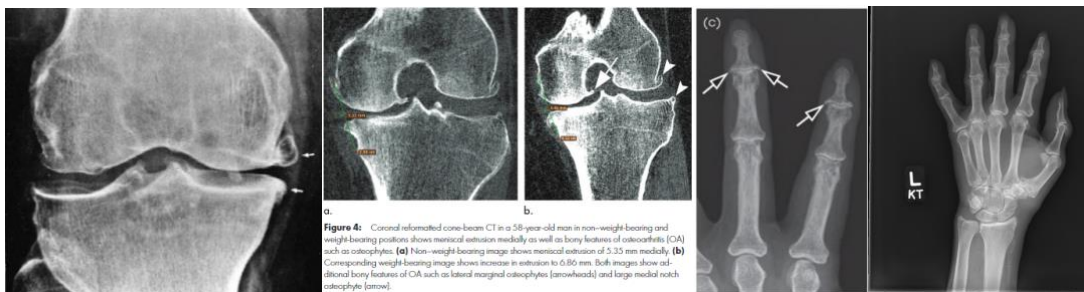


Figure 4: Coronal reformatted cone-beam CT in a 58-year-old man in non-weight bearing and weight-bearing positions shows meniscal extrusion medially as well as bony features of osteoarthritis (OA) such as osteophytes. (a) Non-weight bearing image shows meniscal extrusion of 5.33 mm medially. (b) Corresponding weight-bearing image shows increase in extrusion to 6.55 mm. Both images show additional bony features of OA such as lateral marginal osteophytes (arrowheads) and large medial notch osteophyte (arrow).

Image source(s): Left - Strickland, 2014; Center Left - Roemer et al., 2020; Center Right - Taljanovic et al., 2019; Right - [Radiopaedia](#)

Osteophytes and sclerotic activity

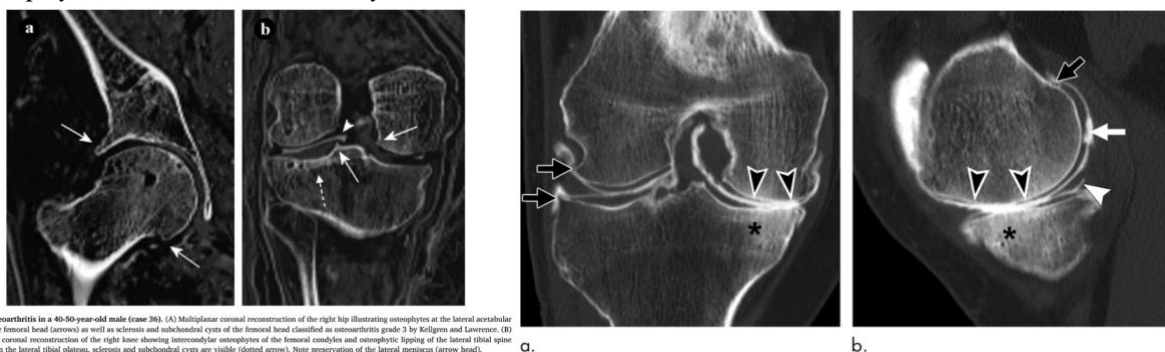


Fig. 2. Osteoarthritis in a 40-50-year-old male (case 36). (A) Multiplanar coronal reconstruction of the right hip illustrating osteophytes at the lateral acromioclavicular joint and the femoral head (arrows) as well as sclerosis and subchondral cysts of the femoral head (classified as osteoarthritis grade 3 by Kellgren and Lawrence). (B) Multiplanar coronal reconstruction of the right knee showing intercondylar osteophytes of the femoral condyles and osteophytic lipping of the lateral tibial spine (arrows). On the lateral tibial plateau, sclerosis and subchondral cysts are visible (dotted arrow). Note preservation of the lateral meniscus (arrow head).

Image source(s): Left and Center Left - Roemer et al., 2020: *=subchondral sclerosis, black arrows=osteophytes; Center Right and Right - Panzer et al., 2021: Arrows= osteophytes, dotted arrow=sclerosis and subchondral cysts

Porosity/Erosion

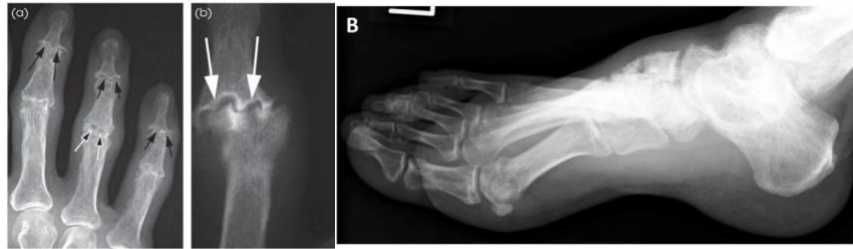


Image source(s): Left and Center - Taljanovic et al., 2019; Right - Kanzaki et al., 2011



Image source(s): Left and Center Left - Kanzaki et al., 2011; Center Right and Right - Scutellari and Orzincolo, 1998

Sclerosis

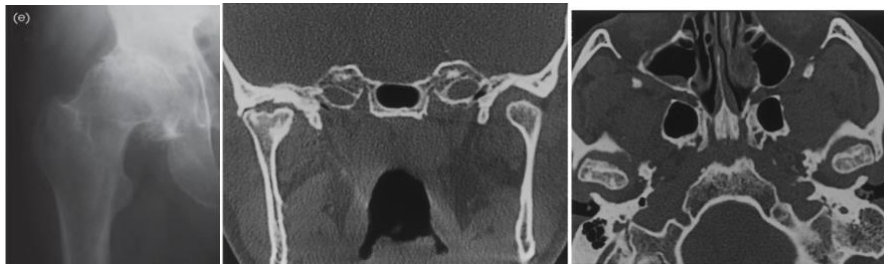


Image source(s): Left - Taljanovic et al., 2019: Acetabular sclerosis; Center and Right - Scutellari and Orzincolo, 1998: Erosion and sclerosis of the condyles

Eburnation

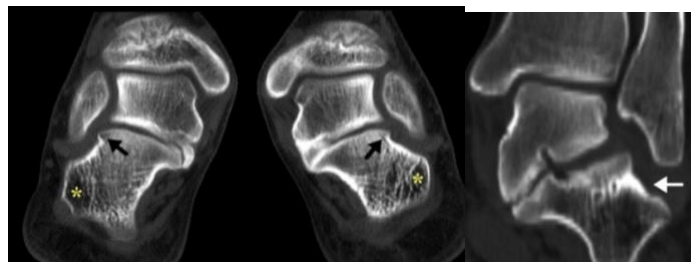


Image source(s): Kernbach and Blitz, 2008: Eburnation is immediately inferior to to the black arrows in association with slight lipping and at the site of the white arrow.

24. Vertebral Osteoarthritis

Alternate name: Vertebral osteophytosis (when of the centrum)

Reference(s): [Normal cervical vertebrae](#), [Normal thoracic vertebrae](#), [Normal lumbar vertebrae](#)

Zygapophyses/Intervertebral facets

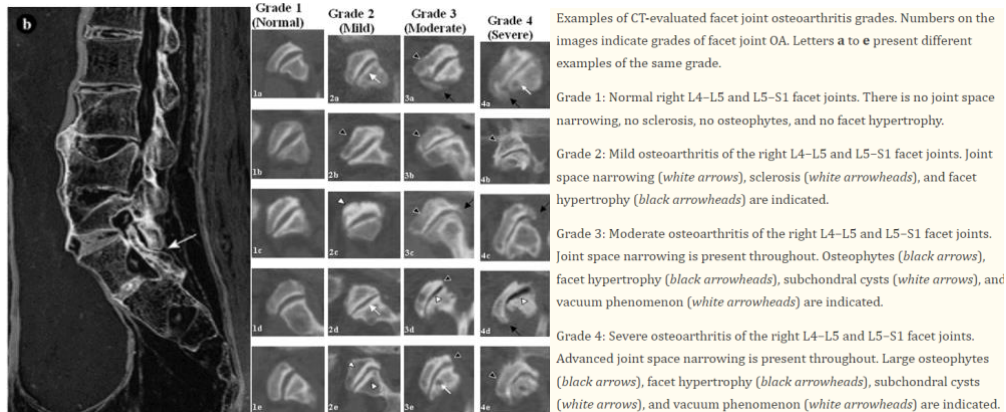


Image source(s): Left - Panzer et al., 2021: Osteophytic growth, bony deformation, bony fusion of facets L5-S1, Arrow= sclerosis of left facet between L4-L5; Center and Right - Kalichman et al., 2009

Centrum

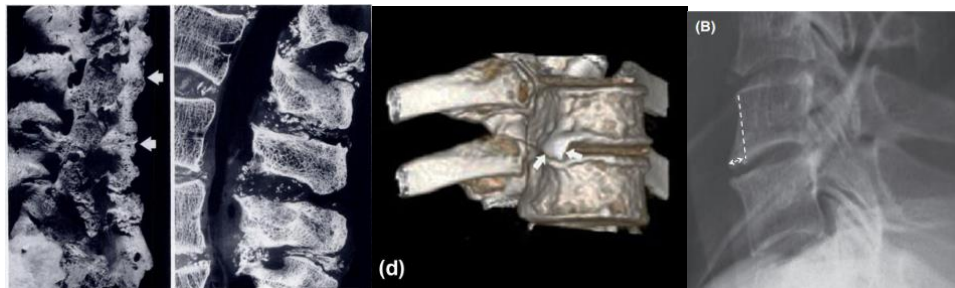


Image source(s): Left and Center Left - Sartoris et al., 1985: White arrows point to osteophytes; Center Right - Kacar et al., 2017; Right - van Eerd et al., 2021

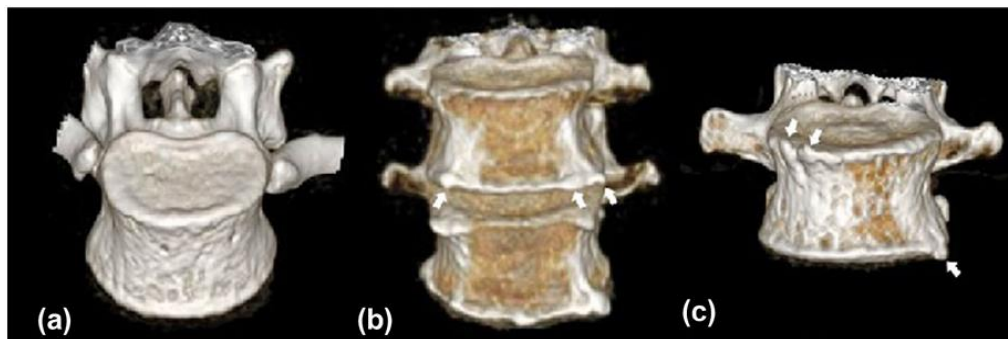


Image source(s): Kacar et al., 2017

Spinous processes

Only record as OA with pseudoarthrosis, record as enthesopathy otherwise

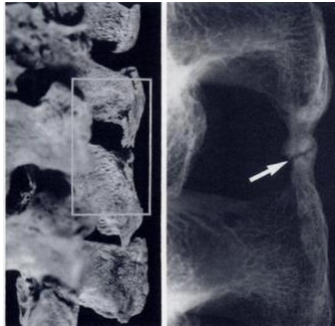


Image source(s): Sartoris et al., 1985; Left - on bone; Right - on CT

Transverse processes



Fig. 19—81-year-old man with Paget disease. Axial CT scan shows increased density, enlargement, and cortical thickening of posteromedial aspect of left ninth rib and secondary degenerative arthritis of costovertebral and costotransverse articulations. Abnormal radiotracer uptake at corresponding site was seen on bone scintigraphy.

Image source(s): Left - Levine et al., 2009; Center Left, Center Right, and Right - Iwasaki et al., 2017: Osteophytes on centrum and transverse processes. Transverse processes osteophytes noted with red arrows.

25. Schmorl's Nodes

Alternate names: Schmorl's depressions; Schmorl's nodules

Definition(s): "Schmorl's nodes occur as a result of intervertebral disk pressure on the superior or inferior surfaces of the vertebral bodies...Schmorl's nodes are commonly associated with other forms of degenerative change, such as the formation of bony spurs or osteophytes extending from the vertebral bodies (Buikstra and Ubelaker, 1994, p. 121)."



Image source(s): Liu et al., 2018, Figure 1: Schmorl's nodes (SNs) on radiographs, computed tomography (CT), and MRI. There are usually multiple lesions in the same individual. In sagittal images, SNs are more commonly located at the middle portion of the vertebral bodies.

26. Spina Bifida

Alternate name(s): neural arch defects, failures of neural tube closure

Definition(s): Non-fusion of sacral arches for sacral units [at or above] S4 (Buikstra and Ubelaker, 1994, p. 122).

Preferred viewing modality: transverse.

Sacral: specify level of closure (ex., at the level of L5 in this individual),

Cervical, Thoracic, Lumbar, Isolated: specify affected vertebrae (ex., C1 in this individual)

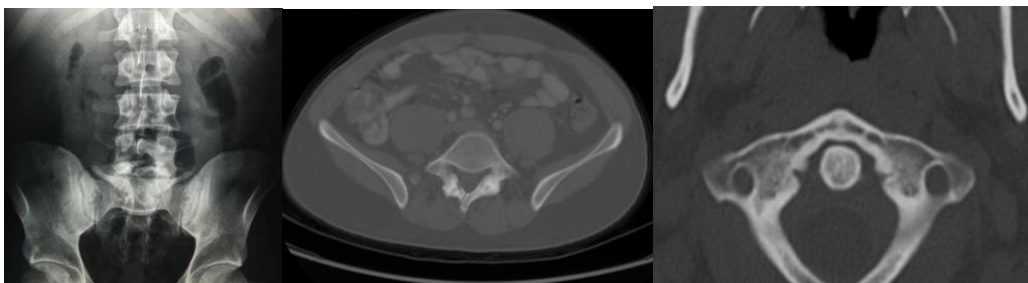


Image source(s): Radiopaedia - [Left](#), [Center](#); Wikipedia - [Right](#)

27. Ankylosing Spondylitis

Definition(s): Ankylosing spondylitis (AS)...is a progressive inflammatory disorder that primarily affects the axial skeleton, including the sacroiliac joints. AS alters the biomechanical properties of the spine through a chronic inflammatory process that causes intravertebral bone loss and bone erosions, followed by the triggering of new bone formation. This multistep process results in a structural damage of bone and leads to an increased risk of vertebral fractures, even from minor injury (Leone et al., 2016, p. 1335).

A form of arthritis which, in contrast to severe OA, manifests as erosion/structural weakness (may be accompanied by fractures), ossification of connective tissue (including ligaments, discs, disc spaces, apophyses), and sclerotic reaction (Radiopaedia).

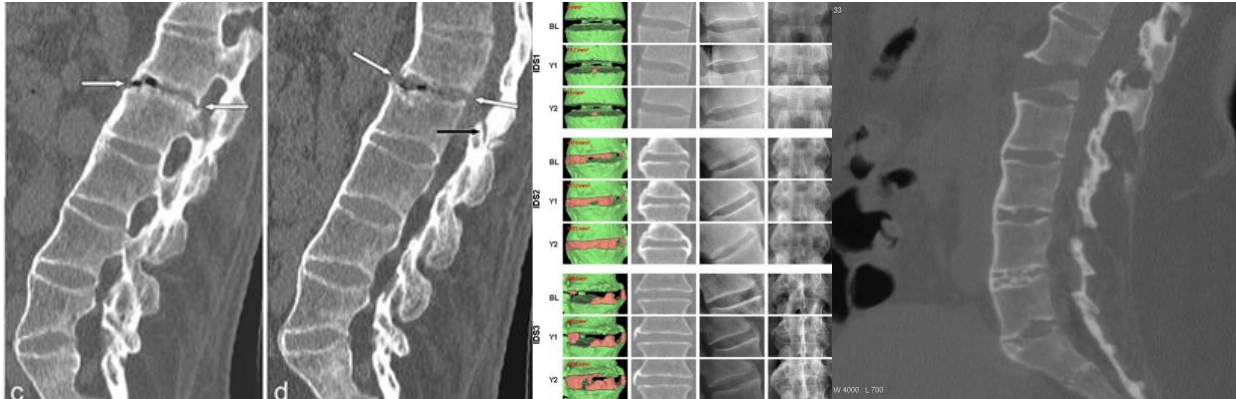


Image source(s): Left and Center Left - Leone et al., 2016: (c) and (d) AS with fractures; Center Right and Right - Tan et al., 2015; Right - [Radiopaedia](#)



Fig. 21—Ankylosing spondylitis in 42-year-old woman. Axial CT scan shows subchondral erosions, irregularity, and sclerosis of both costovertebral joints that is more pronounced on vertebral side of joints. Note erosion and reactive sclerosis along anterior surface of vertebral body (Romanus lesion).

Image source(s): Levine et al., 2008

28. Curvature of Spine

2 measurement modalities: side-to-side (viewed anterior/posterior) or front-to-back (view medial/lateral)

Scoliosis

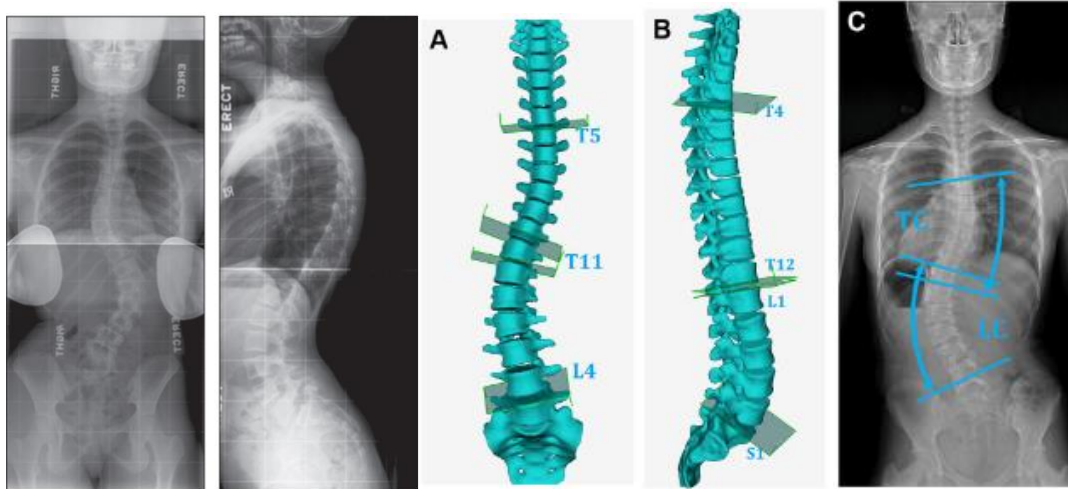


Image source(s): Left and second from Left - Malfair et al., 2010; Center, second from Right, and Right - Zhang et al., 2022 (a), (b), (c)

Cervical Lordosis

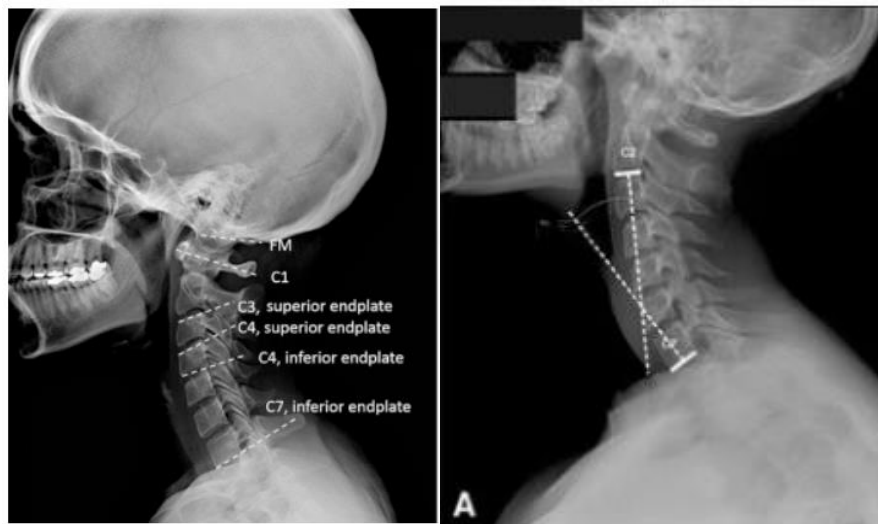


Image source(s): Left - Been et al., 2017; Right - Janusz et al., 2015

Thoracic Kyphosis

Alternate name(s): Hyperkyphosis since some amount of kyphosis is normal.

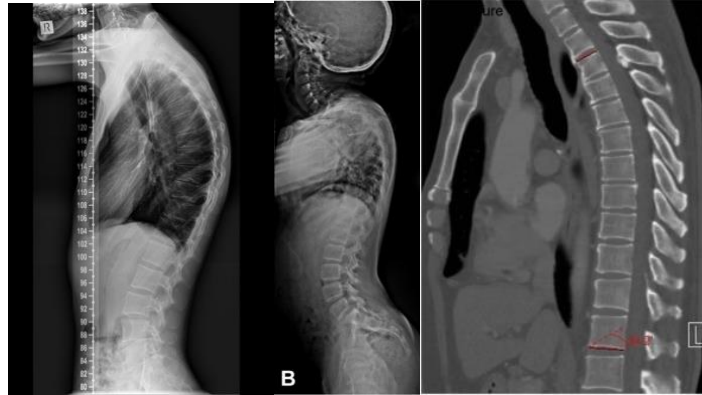


Image source(s): Left - [Radiopaedia](#); Center - Rajasekaran et al., 2018; Right - Kim et al., 2018

Lumbar Lordosis

Alternate name(s): Lumbar hyperlordosis since a range of lumbar lordosis is normal.



Image source(s): Left - Cho et al., 2019; Right - Russel et al., 2020

Loss of Lordosis

Alternate name(s): flat-back



Image source(s): Harrison and Oakley, 2018: The vertical black line represents the ideal sagittal alignment of the posterior inferior body of T12 relative to the origin at the posterior inferior body of S1. The black ellipse represents the ideal curvature of the posterior vertebral body margins of L1–L5. The black line at the posterior body margins of L1–L5 represents the patient’s lumbar curvature.

29. Atherosclerosis Calcification

Definition(s): Calcification plaques at the major coronary arteries. Will only be able to identify calcification areas of 1.03 to 1.37 mm² in size (Otsuka et al., 2014).

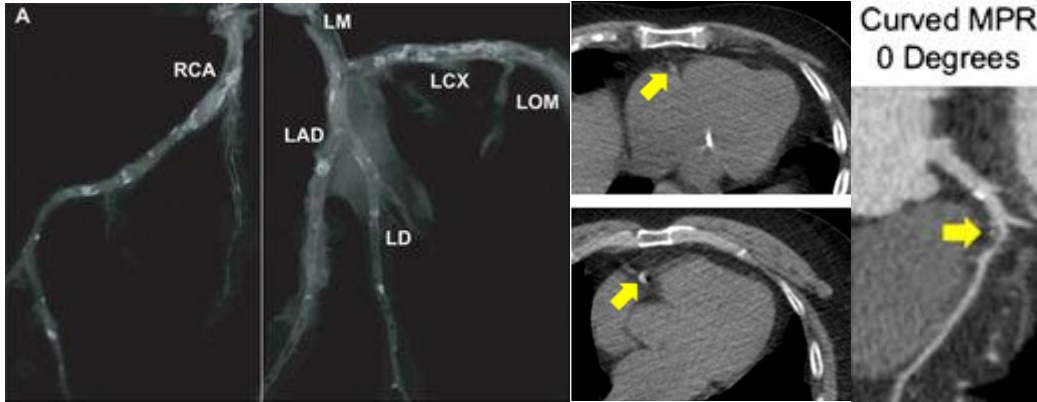


Image source(s): Left - Otsuka et al., 2014; Center and Right - Bailey et al., 2016

30. Pleural Rib Lesions

Pulmonary infections (e.g., tuberculosis) and metastatic cancers can leave proliferative or lytic lesions on ribs. These are often on the pleural or lung surface of the ribs.



Fig. 11—Enchondroma in 60-year-old man. Axial CT scan shows well-circumscribed focus of radiolucency in lateral aspect of rib and mild focal expansion (*arrow*). Absence of cortical breakthrough or thickening, endosteal scalloping, and periosteal reaction suggests benignancy.

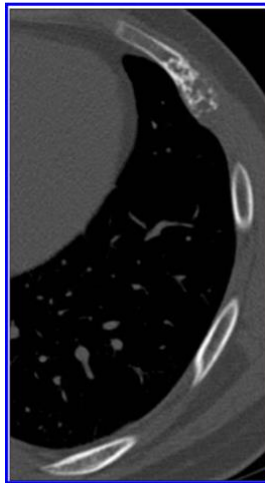


Fig. 10—Low-grade chondrosarcoma in 29-year-old man. Axial CT scan shows mildly expansile lesion of anterior part of left fifth rib. Typical features of cartilage calcification are shown here by stippled ring and arc type pattern.

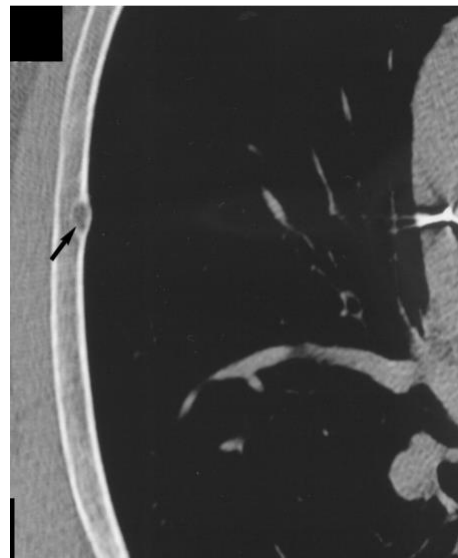


Fig. 10—Rib metastasis in 74-year-old man. CT image shows subtle area of lytic cortical destruction (*arrow*).

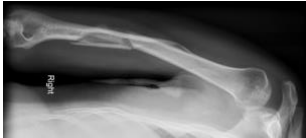
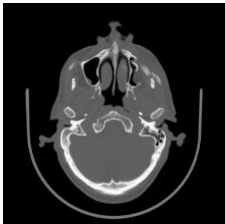
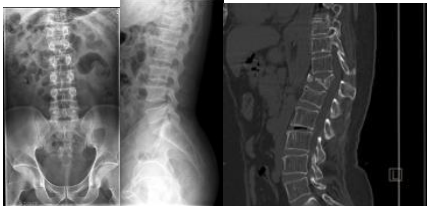
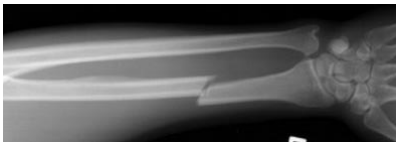
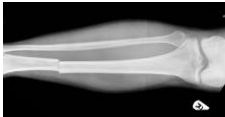
Image source(s): Left/Ctr - Levine et al., 2009; Right:
<https://ajronline.org/doi/full/10.2214/ajr.182.1.1820173>


Trauma and Surgery

31. Fractures




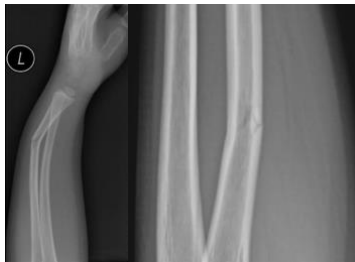
Types of Fractures

(Definitions based on White et al., 2012, unless otherwise noted)

Type	Definition	Image	Image source(s)
Comminuted	The break produces several (three or more) pieces of bone or fragments.		Radiopaedia
Complex	Multiple fractures within the given area that cannot be individually separated out.		Radiopaedia
Compression	Bone tissue collapses (common in vertebrae)		Left & Center Left - Radiopaedia ; Right - Radiopaedia
Simple	A single discontinuity along one line produces two bone segments		Radiopaedia
Transverse	A clean, square break perpendicular to the bone's long axis		Radiopaedia

Depressed	Pushed in with fragments of bone depressed below the adjacent surface		Radiopaedia
-----------	---	--	-----------------------------

Eponym Fractures

Type	Definition	Image	Image source(s)
Parry	An isolated fracture of the ulnar shaft		Hermans et al. 2021
Boxer	Minimally comminuted, transverse fractures of the 5th metacarpal neck		Radiopaedia
Colle's	Distal radius fracture with dorsal comminution, dorsal angulation, dorsal displacement, radial shortening, and an associated fracture of the ulnar styloid		Summers and Fowles 2022
Greenstick	The bone bends on one side and breaks on the other like a bent green tree branch (most common in children)		Radiopaedia - Left , Right

Antemortem/Perimortem



Image source(s): [Radiopaedia](#); Left - Antemortem right femoral fracture; Center Left - Antemortem fracture of left scaphoid resulting in pseudoarthrosis and nonunion; Center Right - Nonunion and pseudoarthrosis following complete antemortem transverse fracture of right tibia and fibula, not set properly; Right - Extensive healing of antemortem fracture to right fifth metacarpal with malunion or non-anatomical angulation



Image source(s): [Radiopaedia](#): Progression of transverse fracture of proximal end of left scaphoid



Image source(s): [Pediatric Radiology](#): Salter-Harris fracture of various growth plates



Image source(s): [CT is us](#): Hematoma of right acetabulum and dislocation of right femoral head

Surgical Intervention



Image source(s): [Radiopaedia](#): Intramedullary nails for an older proximal diaphyseal fracture and posterior dislocation of right femur. No fracture to right acetabulum.

32. Dislocations



Image source(s): Radiopaedia; [Left](#) - Right capitate is dislocated distally and not sitting within the distal articular surface of lunate. Note the space between the proximal surface of right lunate and the distal end of right radius; [Right](#) - Left humeral head is dislocated inferiorly and anteriorly to the glenoid fossa.

33. Surgical Intervention

Pins and wires

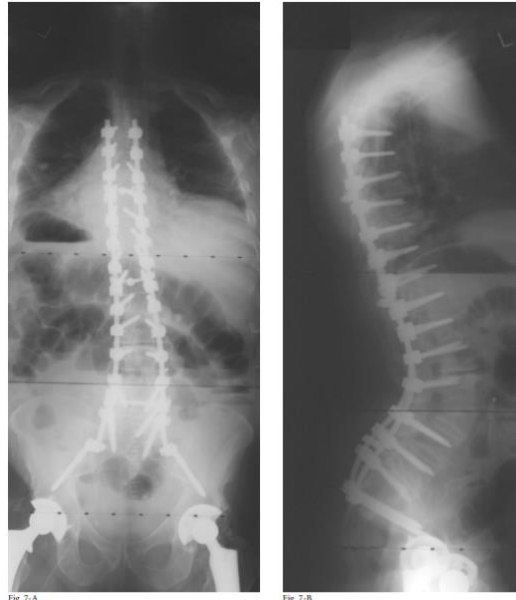


Image source(s): Left and Center - Potter and Lenke, 2004, Figure 7: Anteroposterior and lateral views after operation (pedicle subtraction osteotomy) at L3 fusion mass in a “flat-back” patient.

Screws



Image source(s): [Radiopaedia](#): Complete pelvic resection of the right ilium. Surgical screws stabilizing the right ilium to the sacrum and right acetabulum.

Plates and screws

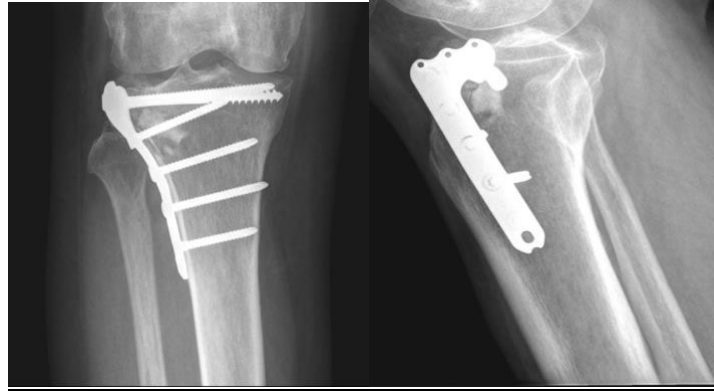


Image source(s): [Radiopaedia](#): Left - Anterior view; Right: Medial view of right tibia with lateral tibial plateau fracture with open reduction and internal fixation by plates and screws

Shunts

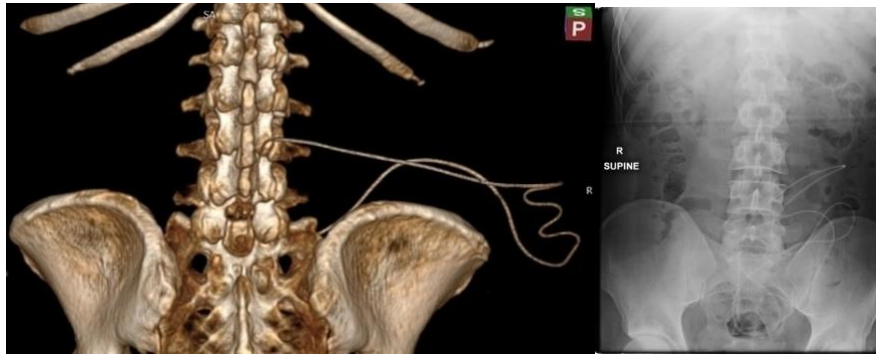


Image source(s): Radiopaedia: [Left](#) - Lumboperitoneal shunt that connects lumbar spinal subarachnoid space to the peritoneal cavity; [Right](#) - Tubing coiled within abdominal cavity.

Ports

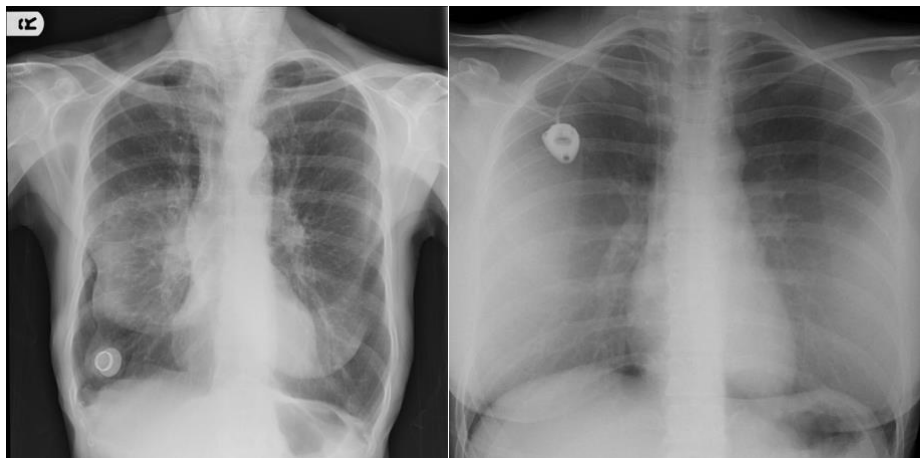


Image source(s): Radiopaedia: [Left](#) - Right breast implant; [Right](#) - Chest port following proper insertion

Intramedullary rod and pins

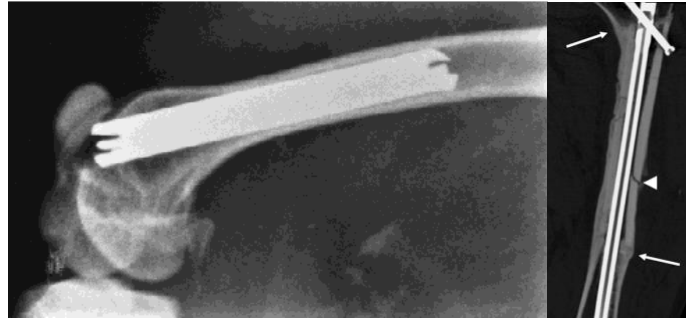


Image source(s): Left - Viljanen et al., 1998, Figure 1b: Lateral view of intramedullary rod locked in by pins; Right - Vande Berg et al., 2006

Implants



Image source(s): Radiopaedia: [Left](#) - Anterior wireless intracranial pressure monitor with a posterior ventriculoperitoneal shunt; [Center](#) - Wireless pacemaker shaped a small rod or pill; [Right](#) - Right sided pacemaker “box”

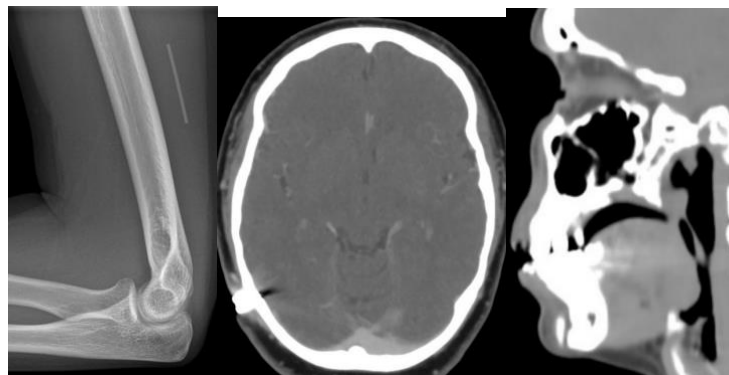


Image source(s): Radiopaedia: [Left](#) - Left arm with a linear dense foreign body in soft tissue of the medial and distal aspects. Object is an implantable contraceptive device; [Center](#) - Inferior to the right parietal bone is a metal bone-anchored hearing aid; [Right](#) - Chin implant

Standards

34. Craniofacial Asymmetry

Note that data on craniofacial asymmetry are not currently being collected by the UWF Biocultural Lab. However, we recognize the importance of these traits to understanding embodied experiences of childhood stress, continue to work toward CT-based protocols for assessing them, and encourage the collection of these data by others.

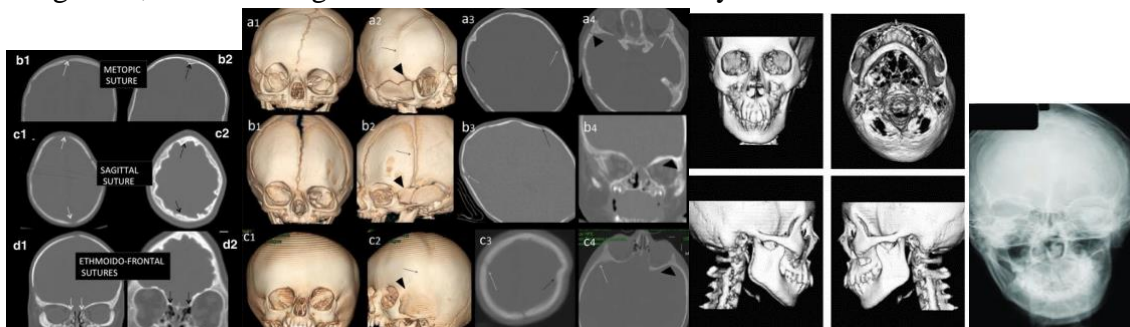


Image Sources: Calandrelli et al., 2014; Park et al., 2006; Jayaratne et al., 2010

35. Basion-Bregma Height

Distance starting at the basion (ba), or the craniometric landmark defined as “[t]he midline point on the anterior margin of the foramen magnum. For cranial height measurements, the point is placed on the anteroinferior portion of the foramen’s rim,” and the bregma (b) is defined as “[t]he ectocranial midline point where the coronal and sagittal sutures intersect” (Buikstra and Ubelaker, 1994, p. 72-73).

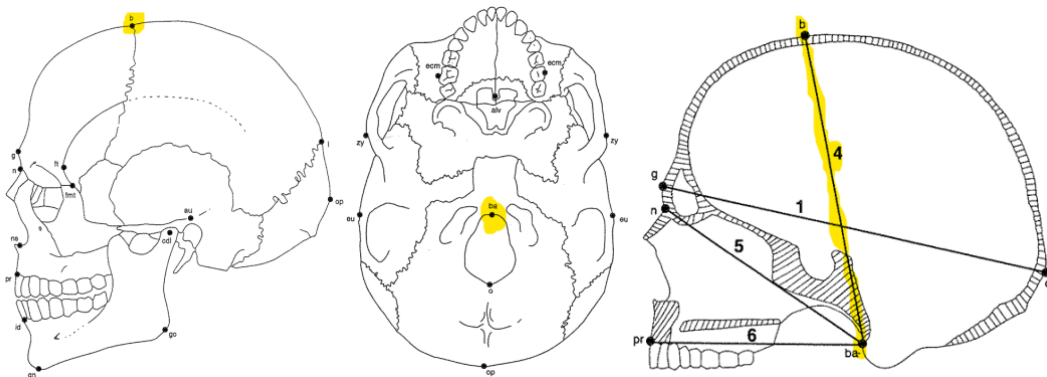


Image source(s): Buikstra and Ubelaker, 1994

36. Maximum Fibula Length

Maximum distance between the most superior point on the fibula head and the most inferior point on the lateral malleolus (Buikstra and Ubelaker, 1994, p. 84).

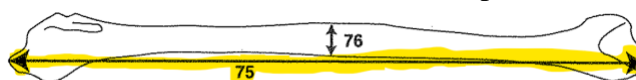


Image source(s): Buikstra and Ubelaker, 1994

37. Femur Midshaft Diameter

This will be an approximate measure due to difficulties in visualizing the entire bone in medicolegal CT scans. Take measurement at the point with roughly the broadest diameter, usually medial-lateral (Buikstra and Ubelaker, 1994, p. 83).

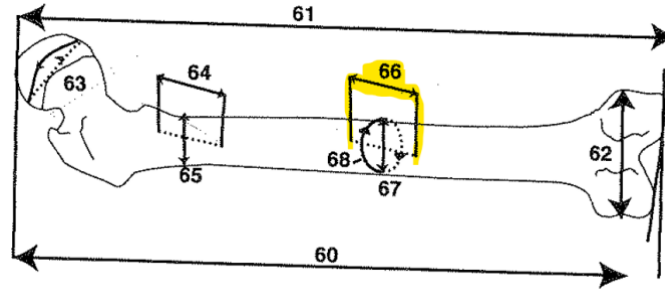
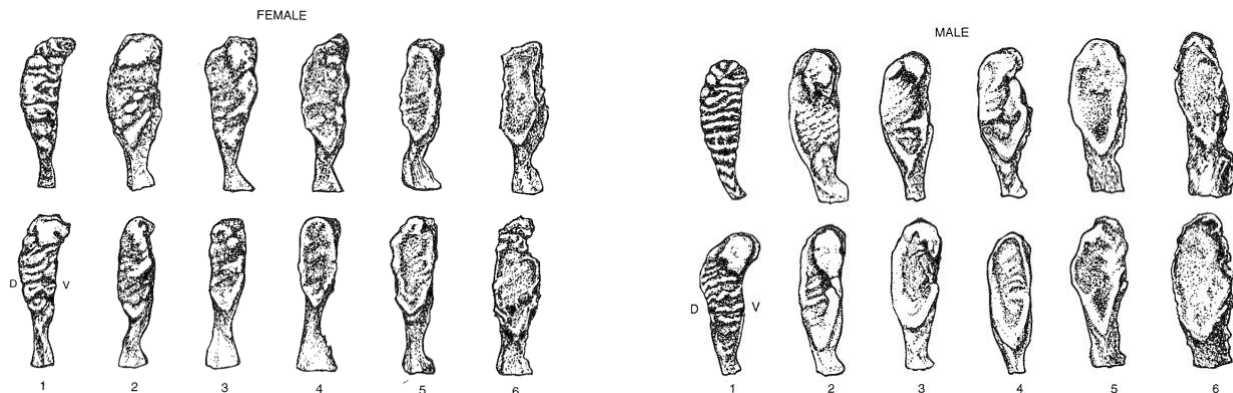


Image source(s): Buikstra and Ubelaker, 1994

38. Pubic Symphysis (Brooks and Suchey 1990)

Suchey Brooks (Buikstra and Ubelaker, 1994, p. 23-24)

- Phase 1.* Symphyseal face has a billowing surface composed of ridges and furrows which includes the pubic tubercle. The horizontal ridges are well-marked. Ventral beveling may be commencing. Although ossific nodules may occur on the upper extremity, a key feature of this phase is the lack of delimitation for either extremity (upper or lower).
- Phase 2.* Symphyseal face may still show ridge development. Lower and upper extremities show early stages of delimitation, with or without ossific nodules. Ventral rampart may begin formation as extension from either or both extremities.
- Phase 3.* Symphyseal face shows lower extremity and ventral rampart in process of completion. Fusing ossific nodules may form upper extremity and extend along ventral border. Symphyseal face may either be smooth or retain distinct ridges. Dorsal plateau is complete. No lipping of symphyseal dorsal margin or bony ligamentous outgrowths.
- Phase 4.* Symphyseal face is generally fine-grained, although remnants of ridge and furrow system may remain. Oval outline usually complete at this stage, though a hiatus may occur in upper aspect of ventral circumference. Pubic tubercle is fully separated from the symphyseal face through definition of upper extremity. Symphyseal face may have a distinct rim. Ventrally, bony ligamentous outgrowths may occur in inferior portion of pubic bone adjacent to symphyseal face. Slight lipping may appear on dorsal border.
- Phase 5.* Slight depression of the face relative to a completed rim. Moderate lipping is usually found on the dorsal border with prominent ligamentous outgrowths on the ventral border. Little or no rim erosion, though breakdown possible on superior aspect of ventral border.
- Phase 6.* Symphyseal face shows ongoing depression as rim erodes. Ventral ligamentous attachments are marked. Pubic tubercle may appear as a separate bony knob. Face may be pitted or porous, giving an appearance of disfigurement as the ongoing process of erratic ossification proceeds. Crenulations may occur, with the shape of the face often irregular.



39. Acetabular Rim Traits (SanMillán et al., 2017)

Variable 1

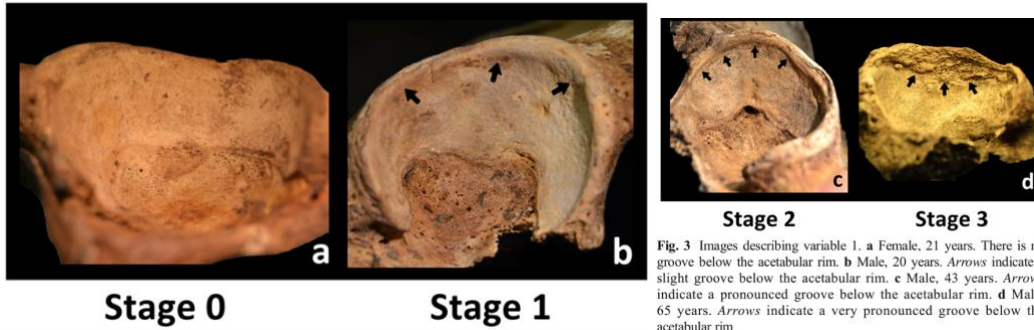


Fig. 3 Images describing variable 1. a Female, 21 years. There is no groove below the acetabular rim. b Male, 20 years. Arrows indicate a slight groove below the acetabular rim. c Male, 43 years. Arrows indicate a pronounced groove below the acetabular rim. d Male, 65 years. Arrows indicate a very pronounced groove below the acetabular rim

1: Acetabular groove (Fig. 3)	This groove appears below and surrounds the internal margin of the acetabular rim. With age, the acetabular groove can become more or less pronounced either along the entire acetabular rim or along only a part of it.	No groove	There is no groove below the acetabular rim. There is no anatomical interruption between the lunata surface and the acetabular rim (Fig. 3a).	0
		Groove	An anatomical interruption is observed between the lunata surface and the acetabular rim. Although it might be short or shallow, it surrounds some or much of the acetabular rim (Fig. 3b).	1
		Pronounced groove	A deeper groove surrounds a large part of the acetabular rim (Fig. 3c).	2
		Very pronounced groove	An extremely pronounced groove surrounds nearly all the acetabular rim. In some specimens, extreme growth of the rim has obscured the groove so that only a tissue discontinuity between the lunata surface and the acetabular rim can be observed (Fig. 3d).	3

Variable 2

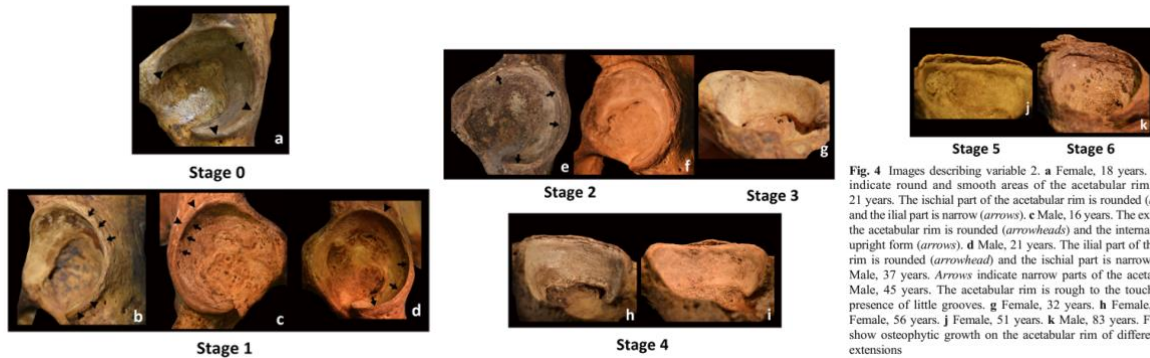
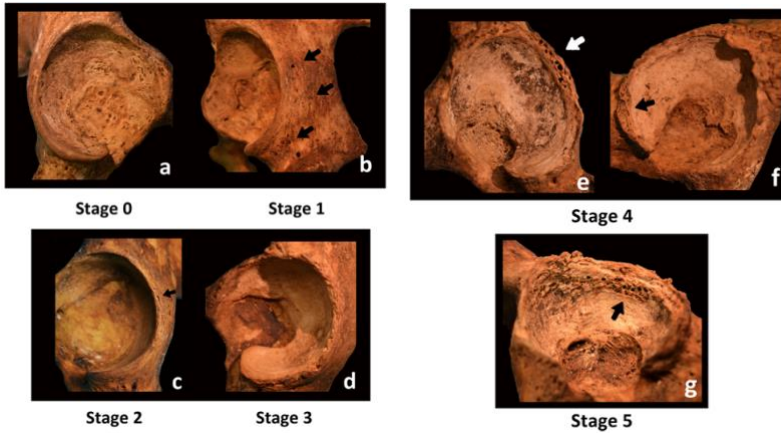


Fig. 4 Images describing variable 2. a Female, 18 years. Arrowheads indicate round and smooth areas of the acetabular rim. b Female, 21 years. The ischial part of the acetabular rim is rounded (arrowheads) and the iliac part is narrow (arrows). c Male, 16 years. The external part of the acetabular rim is rounded (arrowheads) and the internal part has an upright form (arrows). d Male, 21 years. The iliac part of the acetabular rim is rounded (arrowhead) and the ischial part is narrow (arrows). e Male, 37 years. Arrows indicate narrow parts of the acetabular rim. f Male, 45 years. The acetabular rim is rough to the touch due to the presence of little grooves. g Female, 32 years. h Female, 61 years. i Female, 56 years. j Female, 51 years. k Male, 83 years. Figures (g-k) show osteophytic growth on the acetabular rim of different sizes and extensions

2: Acetabular rim shape (Fig. 4)	With age, the acetabular rim loses its round and smooth form as a consequence of the progressive development of osteophytes, which can become a crest.	Rounded acetabular rim	The acetabular rim is dense, round, and smooth, typical of young specimens (Fig. 4a).	0
		Partially narrow acetabular rim	The acetabular rim keeps its round and smooth form in some areas, but in others is narrower. There are three possibilities: (a) the iliac part of the acetabular rim narrows, but not the ischial part (Fig. 4b); (b) the external part of the acetabular rim retains its rounded form, but its internal part has an upright form (Fig. 4c); or (c) the ischial part of the acetabular rim narrows, but not the iliac part (Fig. 4d). In all of these cases, the acetabular rim is smooth to the touch.	1
		Narrow or rough acetabular rim	There are two possibilities: (a) whole or most of the acetabular rim is narrow (Fig. 4e), or (b) some part of the acetabular rim might be rough to the touch due to the presence of little grooves (Fig. 4f). In both possibilities, there is no osteophytic construction.	2
		Partially crested rim	Osteophytic constructions form a small chain (≈ 1 mm in height) on some small part of rim (Fig. 4g); a bigger osteophyte linked or not to the chain might be observed.	3
		Crested rim	An osteophytic formation makes either (a) a low crest (≈ 1 mm in height) along the entire acetabular rim (Fig. 4h) or (b) a high crest (2–3.9 mm in height) along only part of the acetabular rim (Fig. 4i). This crest usually appears dense, but not always .	4
		Very high crested rim	A very high crest (≥ 4 mm in height) has developed as a consequence of bone construction and destruction (Fig. 4j). This crest is thin and sharp or rounded with a spongy appearance.	5
		Destructured rim	An extremely high crest (≥ 8 mm in height) has developed (Fig. 4k). It may be either thin and sharp and leaning slightly toward the lunata surface or rounded, spongy, and fragile with swollen and hollow bone.	6

Variable 3



◀ Fig. 5 Images describing variable 3. a Male, 16 years. The acetabular rim is smooth without porosities and roughness. b Male, 18 years. Arrows indicate microporosity increased lightly on the area around the acetabulum. e Female, 24 years. Arrow indicates some microporosities on the acetabular rim, but it keeps a round and dense appearance. d Male, 67 years. The acetabular rim is not smooth to the touch. e Female, 85 years. Arrow indicates newly constructed bone with many micro- and macroporosities, suffering subsequent destruction. f Female, 82 years. Arrow indicates the area of the acetabular rim which has suffered bone destruction through micro- and macroporosities. g Female, 94 years. Arrow shows the place where macro- and microporosities of the destructured acetabular rim have partially invaded the lunata surface

3: Acetabular rim porosity (Fig. 5)	With aging, porosity appears on the acetabular rim and on the adjacent ilio-ischial area of the acetabulum. Two kinds of porosity can be defined: (a) microporosity, which refers to a fine, just optically visible perforation (≤ 1 mm), and (b) macroporosity, which refers to an oval or round perforation larger than 1 mm.	Normal porosity	Acetabular rim is smooth without porosities and roughness. The area adjacent to the acetabular rim also has normal porosity (Fig. 5a).	0
		External porosity	On the area around the acetabulum, microporosity is lightly increased on the anterior inferior iliac spine, on the posterior wall of the acetabulum, and on the area below the two extremities of the lunata surface. There is no porosity on the acetabular rim, which is dense and smooth (Fig. 5b).	1
		Rim porosities	Some microporosities on the acetabular rim may be large ($=1$ mm), but the acetabular rim always has a round and dense appearance. There is no bone destruction (Fig. 5c).	2
		Rough rim	The acetabular rim is not smooth to the touch (Fig. 5d) and there may be some macroporosity on the rim.	3
		Destructured	Newly constructed bone has become very porous with many micro- and macroporosities (Fig. 5e), or it has suffered subsequent destruction. There is bone destruction, i.e., micro- and macroporosities on the acetabular rim; but not necessarily in the newly constructed bone (Fig. 5f).	4
	Extremely destructured rim	Macro- and microporosities of the destructured acetabular rim have partially invaded the lunata surface. Usually, this invasion occurs on the superior area of the lunata surface, below the anterior inferior iliac spine, or around the ilium-ischium intersection (Fig. 5g).	5	

Variable 4

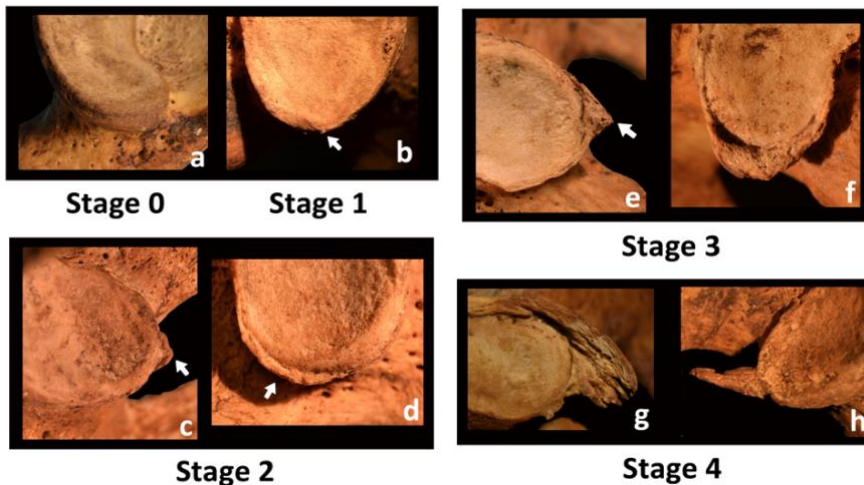


Fig. 6 Images describing variable 4. a Female, 21 years. The apex is round and smooth. b Male, 49 years. Arrow indicates a small bone spicule on the apex. c Female, 56 years. Arrow indicates an osteophyte ≥ 1 mm on the apex. d Female, 76 years. Arrow indicates a bone proliferation ≥ 1 mm, which covers the entire apex. e Male, 82 years. Arrow indicates an osteophyte ≥ 3 mm on the apex. f Female, 83 years. An osteophyte ≥ 3 mm covers the entire horn of the lunata surface. g Male, 68 years. h Male, 65 years. In (g) and (h), an osteophyte ≥ 5 mm is present on the apex

4: Apex activity (Fig. 6)	Apex activity refers to the bone activity observed on the apex of the posterior horn of the lunata surface. With aging, this apex loses its rounded form, gradually becoming sharper and finally developing a spicule, which can become quite large.	No activity	The apex is round and smooth to the touch. There is no spicule (Fig. 6a).	0
		Apex activity	The apex has become longer and is sharp to the touch, or a small spicule can be felt (Fig. 6b). In some cases, there may not be a spicule, but it might be rough to the touch due to the presence of little grooves.	1
		Osteophytic activity (≥ 1 mm)	A developed and conspicuous osteophyte equal to or larger than 1 mm can be seen with the naked eye (Fig. 6c). This bone growth may cover the entire horn (Fig. 6d).	2
		Much osteophytic activity (≥ 3 mm)	The apex has an osteophyte equal to or larger than 3 mm (Fig. 6e), which may cover the entire horn of the lunata surface (Fig. 6f).	3
		Very much osteophytic activity (≥ 5 mm)	An osteophyte is so large (≥ 5 mm) that it enters the acetabular notch (Fig. 6g, h) and may completely cross it, in which case the anterior horn of the lunata surface can also have activity.	4

Variable 5

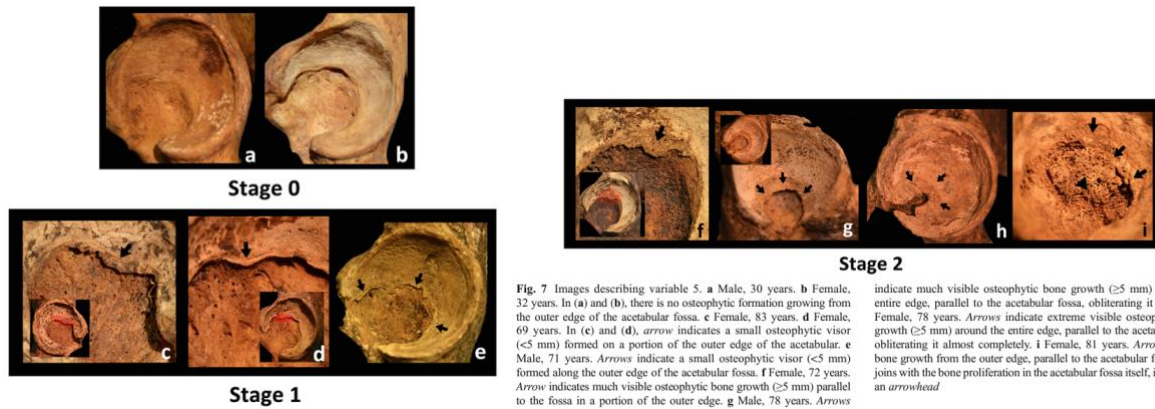
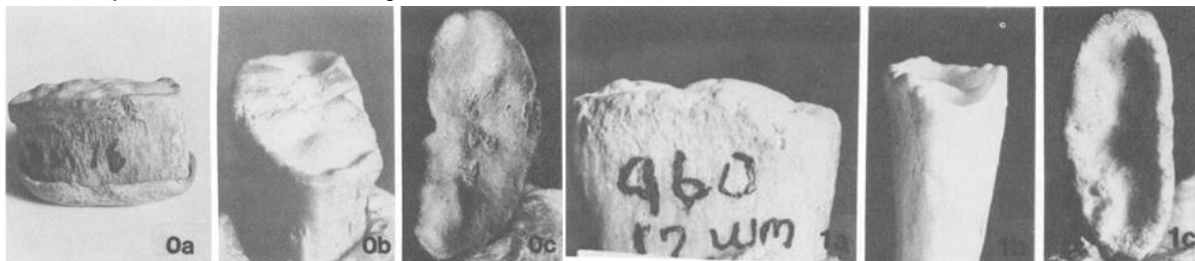


Fig. 7 Images describing variable 5. a Male, 30 years. b Female, 32 years. In (a) and (b), there is no osteophytic formation growing from the outer edge of the acetabular fossa. c Female, 83 years. d Female, 69 years. In (c) and (d), *arrow* indicates a small osteophytic visor (< 5 mm) formed on a portion of the outer edge of the acetabular fossa. e Male, 71 years. *Arrows* indicate a small osteophytic visor (< 5 mm) formed along the outer edge of the acetabular fossa. f Female, 72 years. *Arrow* indicates much visible osteophytic bone growth (≥ 5 mm) parallel to the fossa in a portion of the outer edge. g Male, 78 years. *Arrows* indicate much visible osteophytic bone growth (≥ 5 mm) around the entire edge, parallel to the acetabular fossa, obliterating it partially. h Female, 78 years. *Arrows* indicate extreme visible osteophytic bone growth (≥ 5 mm) around the entire edge, parallel to the acetabular fossa, obliterating it almost completely. i Female, 81 years. *Arrows* indicate bone growth from the outer edge, parallel to the acetabular fossa, which joins with the bone proliferation in the acetabular fossa itself, indicated by an *arrowhead*.

5: Activity on the outer edge of the acetabular fossa (Fig. 7)	This activity refers to a visible osteophytic formation that grows as a usually sharp crest from the outer edge of the acetabular fossa toward and parallel to the acetabular fossa. This growth could be extensive until it obliterates the fossa completely.	No activity	There is no osteophytic formation growing from the outer edge of the acetabular fossa, forward, and parallel to the acetabular fossa (Fig. 7a, b).	0
		Slight activity	Osteophytic constructions form a small visor on the outer edge of the acetabular fossa, parallel to the acetabular fossa. This growth is small (< 5 mm), but it could develop around a portion (Fig. 7c, d) or all of the outer edge of the acetabular fossa (Fig. 7e).	1
		Much activity	There is much visible osteophytic bone growth parallel to the acetabular fossa (≥ 5 mm). This growth can appear around a small part of the outer edge of the acetabular fossa, usually in the superior lobe of the acetabular fossa (Fig. 7f), or around the entire edge (Fig. 7g, h). This bone proliferation may obliterate the acetabular fossa partially (Fig. 7g) or completely (Fig. 7h). Sometimes, this growth can join with bone growth from the acetabular fossa itself (Fig. 7i).	2

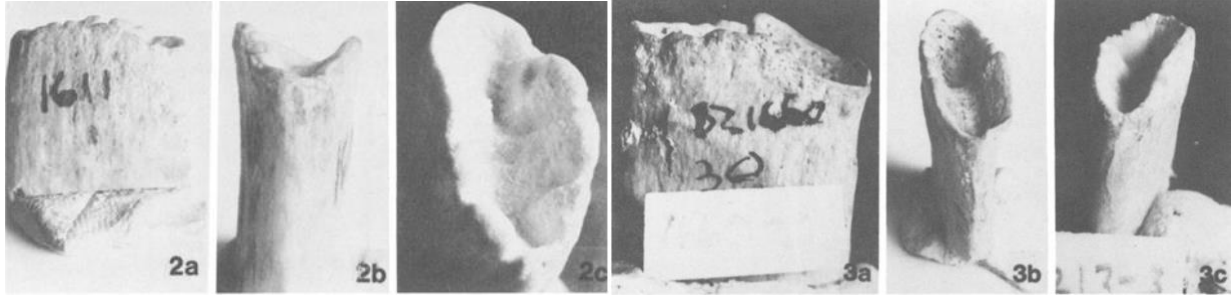
40. Fourth Sternal Rib Ends

Standards for (White) Males (Işcan et al., 1984)



Phase 0: The articular surface is flat or bilowy with a regular rim and rounded edges. The bone itself is smooth, firm, and very solid (Plate 1: Fig. 0a, b, and c).

Phase 1: There is a beginning amorphous indentation in the articular surface, but billowing may also still be present. The rim is rounded and regular. In some cases scallops may start to appear at the edges. The bone is still firm, smooth and solid (Plate 1: Fig. 1a, b, and c).



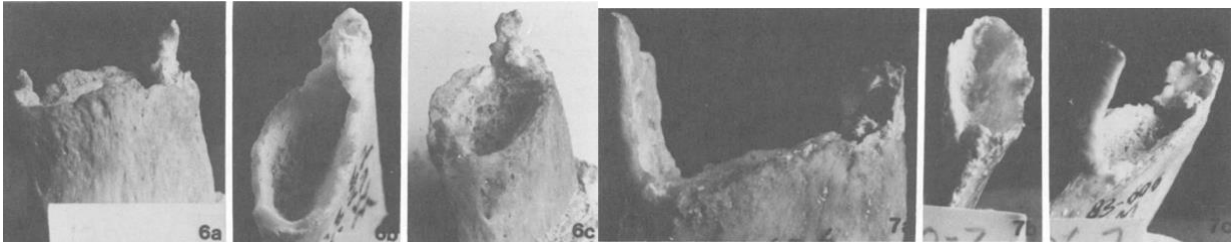
Phase 2: The pit is now deeper and has assumed a V-shaped appearance formed by the anterior and posterior walls. The walls are thick and smooth with a scalloped or slightly wavy rim with rounded edges. The bone is firm and solid (Plate 1: Fig. 2a, b, and c).

Phase 3: The deepening pit has taken on a narrow to moderately U-shape. Walls are still fairly thick with rounded edges. Some scalloping may still be present but the rim is becoming more irregular. The bone is still quite firm and solid (Plate 2: Fig. 3a, b, and c).



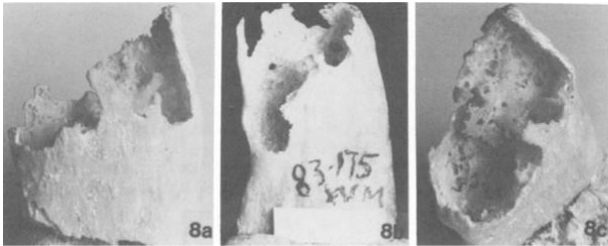
Phase 4: Pit depth is increasing, but the shape is still a narrow to moderately wide U. The walls are thinner, but the edges remain rounded. The rim is more irregular with no uniform

Phase 5: There is little change in pit depth, but the shape in this phase is predominantly a moderately wide U. Walls show further thinning and the edges are becoming sharp. Irregularity is increasing in the rim. Scalloping pattern is completely gone and has been replaced with irregular bony projections. The condition of the bone is fairly good, however, there are some signs of deterioration with evidence of porosity and loss of density (Plate 2: Fig. 5a, b, and c).



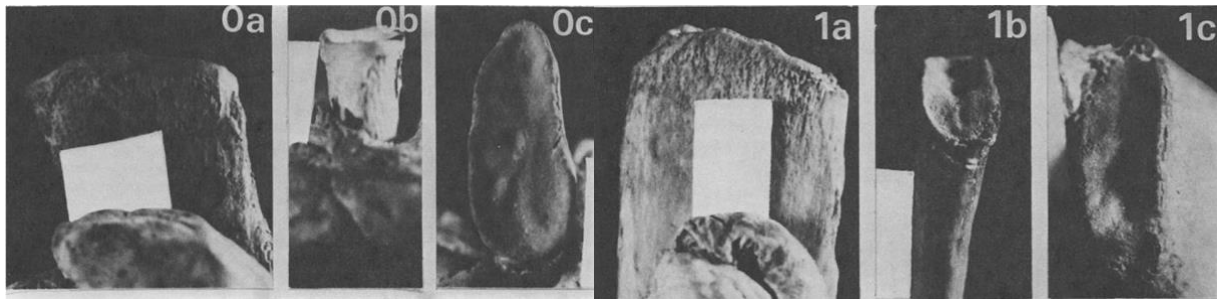
Phase 6: The pit is noticeably deep with a wide U-shape. The walls are thin with sharp edges. The rim is irregular and exhibits some rather long bony projections that are frequently more pronounced at the superior and inferior borders. The bone is noticeably lighter in weight, thinner, and more porous, especially inside the pit (Plate 3: Fig. 6a, b, and c).

Phase 7: The pit is deep with a wide to very wide U-shape. The walls are thin and fragile with sharp, irregular edges and bony projections. The bone is light in weight and brittle with significant deterioration in quality and obvious porosity (Plate 3: Fig. 7a, b, and c).



Phase 8: In this final phase the pit is very deep and widely U-shaped. In some cases the floor of the pit is absent or filled with bony projections. The walls are extremely thin, fragile, and brittle with sharp, highly irregular edges and bony projections. The bone is very lightweight, thin, brittle, friable, and porous. "Window" formation is sometimes seen in the walls (Plate 3: Fig. 8a, b, and c).

Standards for (White) Females (Isçan et al., 1985)

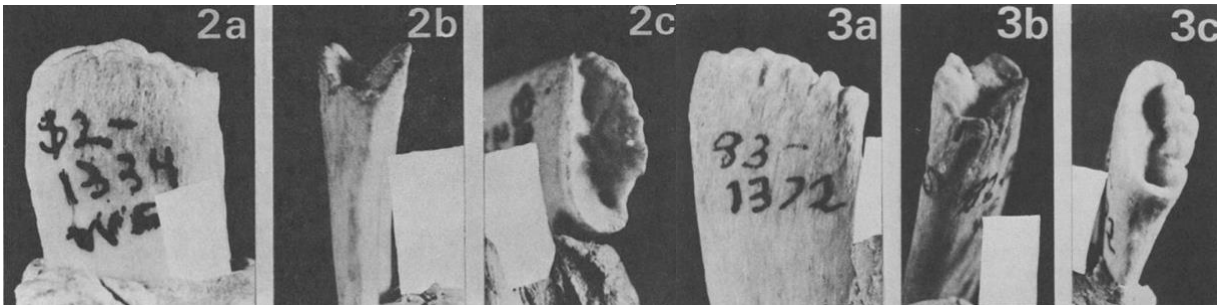


Phase 0

The articular surface is nearly flat with ridges or billowing. The outer surface of the sternal extremity of the rib is bordered by what appears to be an overlay of bone. The rim is regular with rounded edges, and the bone itself is firm, smooth, and very solid (Plate 1: Fig. 0a, b, and c).

Phase 1

A beginning, amorphous indentation can be seen in the articular surface. Ridges or billowing may still be present. The rim is rounded and regular with a little waviness in some cases. The bone remains solid, firm, and smooth (Plate 1: Fig. 1a, b, and c).

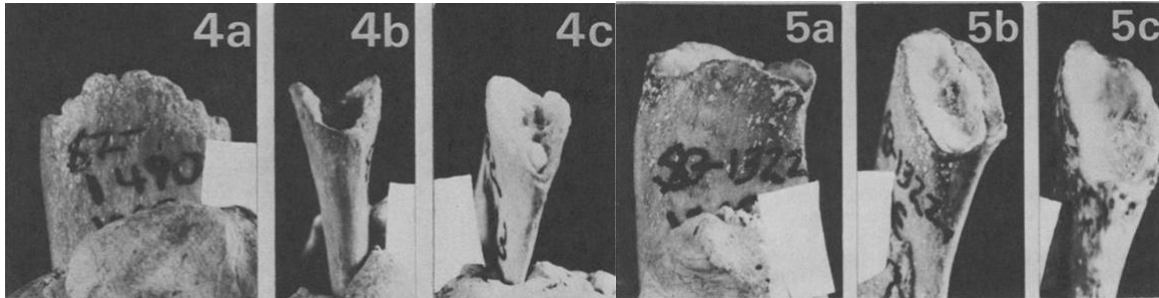


Phase 2

The pit is considerably deeper and has assumed a V-shape between the thick, smooth-walled anterior and posterior walls. Some ridges or billowing may still remain inside the pit. The pronounced, regular scalloping pattern. At this stage, the anterior or posterior walls or both rim is wavy with some scallops beginning to form at the rounded edge. The bone itself is firm and solid (Plate 1: Fig. 2a, b, and c).

Phase 3

There is only slight if any increase in pit depth, but the V-shape is wider, sometimes approaching a narrow U as the walls become a bit thinner. The still rounded edges now show a narrow U. The pronounced, regular scalloping pattern. At this stage, the anterior or posterior walls or both rim is wavy with some scallops beginning to form at the rounded edge. The bone itself is firm and solid (Plate 2: Fig. 3a, b, and c).

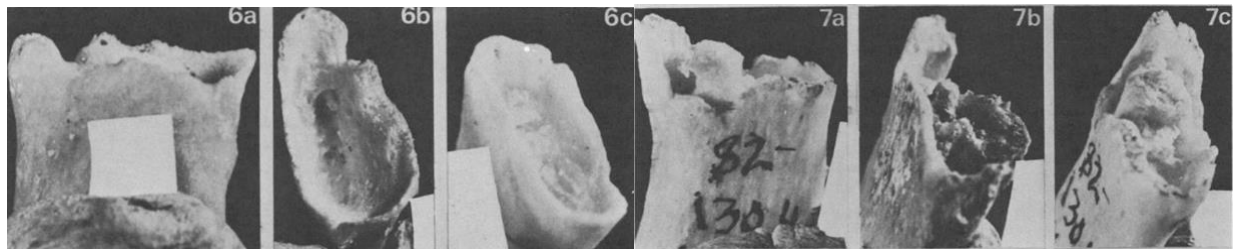


Phase 4

There is a noticeable increase in the depth of the pit, which now has a wide V- or narrow V- or U-shape. In most cases, a smooth, hard, plaque-like deposit lines at least part of the U-shape with, at times, flared edges. The walls are thinner but the rim remains rounded. The rim is well defined and the edges look somewhat worn down. The quality of the bone is noticeably lighter in weight, density and firmness. The texture is somewhat brittle (Plate 2, Fig. 4a, b, and c).

Phase 5

The depth of the pit stays about the same, but the thinning walls are flaring into a wider U-shape with, at times, flared edges. The walls are thinner but the rim remains rounded. The rim is well defined and the edges look somewhat worn down. The quality of the bone is noticeably lighter in weight, density and firmness. The texture is somewhat brittle (Plate 2, Fig. 5a, b, and 5c).

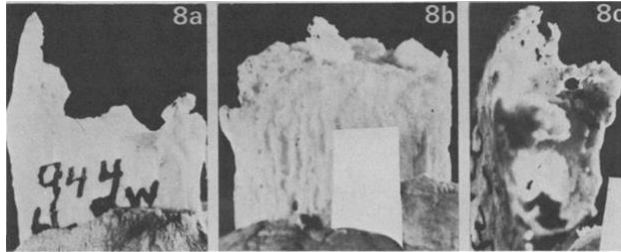


Phase 6

An increase in pit depth is again noted, and its V- or U-shape has widened again because of pronounced flaring at the end. The plaque-like deposit may still appear but is rougher and more porous. The walls are quite thin with sharp edges and an irregular rim. The central arc is less obvious and, in many cases, sharp points project from the rim of the sternal extremity. The bone itself is fairly thin and brittle with some signs of deterioration (Plate 3: Fig. 6a, b, and c).

Phase 7

In this phase, the depth of the predominantly flared U-shaped pit not only shows no increase, but actually decreases slightly. Irregular bony growths are often seen extruding from the interior of the pit. The central arc is still present in most cases but is now accompanied by pointed projections, often at the superior and inferior borders, yet may be evidenced anywhere around the rim. The very thin walls have irregular rims with sharp edges. The bone is very light, thin, brittle, and fragile, with deterioration most noticeable inside the pit (Plate 3: Fig. 7a, b, and c).



Phase 8

The floor of the U-shaped pit in this final phase is relatively shallow, badly deteriorated, or completely eroded. Sometimes it is filled with bony growths. The central arc is barely recognizable. The extremely thin, fragile walls have highly irregular rims with very sharp edges, and often fairly long projections of bone at the inferior and superior borders. "Window" formation sometimes occurs in the walls. The bone itself is in poor condition—extremely thin, light in weight, brittle, and fragile (Plate 3: Fig. 8a, b, and c).

41. Vertebral Neural Canal Dimensions

Measurement should be from the most lateral points on the interior of the canal on either side. Points should be placed at roughly the midpoint of the canal on each vertebra. - For C1 vertebrae, do not include the dens.



Image source(s): Left - De Decker et al., 2010; Center Left, Center Right, and Right - Singh et al., 2016